A new species of *Allodaposuchus* (Eusuchia, Crocodylia) from the late Maastrichtian (Late Cretaceous) of Spain: Phylogenetic and paleobiologic implications.

Alejandro Blanco, Josep Fortuny, Alba Vicente, Àngel H. Lujan, Jordi Garcia-Marçà, Albert Selles

Background. The Late Cretaceous is a keystone period to understand the origin and early radiation of Crocodylia, the group containing all extant lineages of crocodiles. Among the taxa described from the latest Cretaceous of Europe, the genus *Allodaposuchus* is one of the most common but also one of the most controversial. However, because of its fragmentary record, several issues regarding its phylogenetic emplacement and its ecology remain unsolved or unknown. The discovery of a single specimen attributed to *Allodaposuchus*, represented by both cranial and postcranial remains, from the Casa Fabà site (Tremp Basin, NE Spain) in the lower red unit of the Tremp Fm. (late Maastrichtian, Late Cretaceous) offers a unique opportunity to deepen in the phylogenetic relationships of the group and its ecological features. **Methods.** The specimen is described in detail, and CT scan of the skull is performed in order to study the endocranial morphology as well as paratympanic sinuses configuration. In addition, myological and phylogenetic analyses are also carried out on the specimen for to shed light in ecological and phylogenetic issues, respectively. **Results.** The specimen herein described represents a new species, *Allodaposuchus hulki* sp. nov.*,* closely related to the Romanian *A. precedens*. The CT scan of the skull revealed an unexpected paratympanic sinuses configuration. *A. hulki* exhibits an “anterodorsal tympanic sinus” not observed in any other crocodile, nor extant neither extinct taxa. The caudal tympanic recesses are extremely enlarged, and the expanded quadratic sinus seems to be connected to the middle-ear channel. Phylogenetic analyses confirm the emplacement of the informal taxonomic group ‘Allodaposuchia’ at the base of Crocodylia, being considered the sister group of *Borealosuchus* and Planocraniidae. **Discussion.** Although being a preliminary hypothesis, the unique paratympanic configuration displayed by *A. hulki* suggests that it could possess a high-specialized auditory system. Further, the large cranial cavities could also serve as lightening elements of the cranial weight. Concerning the postcranial skeleton, *Allodaposuchus hulki* shows massive and robust vertebrae and forelimb bones, suggesting it could have a bulky body. The myological study performer on the anterior limb elements supports this interpretation. In addition, several bone and muscular features seem to point at a semi-erected position

of the forelimbs during terrestrial locomotion. Taking all the above results, it seems plausible to suggest that *A. hulki* could conduct large incursions out of the water and have a semi-terrestrial lifestyle.

A new species of *Allodaposuchus* (Eusuchia, Crocodylia) from the late Maastrichtian (Late Cretaceous) of Spain: Phylogenetic and paleobiologic implications.

Alejandro Blanco[1], Josep Fortuny[1], Alba Vicente[2], Àngel H. Luján[1], Jordi Alexis Garcia-Marçà[1], Albert G. Sellés[1]*

[1] Institut Català de Paleontologia Miquel Crusafont, Universitat Autònoma de Barcelona, C/ Escola Industrial 23, E-08201, Sabadell, Catalonia, Spain

[2] Departament d'Estratigrafia, Paleontologia i Geociències marines, Facultat de Geologia, Universitat de Barcelona, Carrer de Martí i Franquès s/n, 08028 Barcelona, Catalonia, Spain

*corresponding author: albert.garcia@icp.cat

Introduction

The Late Cretaceous is a crucial period to understand the rise and radiation of Crocodylia. At this time the three main lineages of modern crocodiles make their apparition, and start their dominance upon other crocodilian faunas (Puértolas, Canudo & Cruzado-Caballero, 2011). Thus, any new find regarding the Eusuchia record is worthy because it provides new information to the puzzling origin of modern crocodiles.

In this way, the fossil record of Late Cretaceous crocodilomorphs from Europe offers an exceptional opportunity to approach such questions, because it contains both basal eusuchians and members of all groups involved in the radiation of Crocodylia. In the uppermost Cretaceous strata of SW Europe, basal Eusuchia are represented by the hylaeochampsids *Iharkutosuchus* (Ösi, Clark & Weishampel, 2007), *Acynodon iberoccitanus* (Buscalioni et al., 1997) and *Musturzabalsuchus* (Buscalioni et al., 1997; Narváez et al., 2014). In turn, the clade Alligatoroidea is represented by the genera *Massaliasuchus* (Martin & Buffetaut 2008), whereas *Thoracosaurus* (Laurent, Buffetaut & Le Loeuff, 2000) is included within Gavialoidea, and *Arenysuchus* (Puértolas, Canudo & Cruzado-Caballero, 2011) is considered a basal crocodyloid.

Allodaposuchus Nopcsa 1928 was one of the most common taxon during the latest Cretaceous of Europe, but it is also considered one of the most controversial. Mainly represented by fragmentary skull remains, this genus currently comprises three different species (*A. precedens*, *A. subjuniperus*, and *A. palustris*) reported from Spain (Buscalioni, Ortega & Vasse, 1997; Buscalioni et al., 2001; Puértolas-Pascual, Canudo & Moreno-Azanza, 2013; Blanco et al., 2014), France (Martin, 2010), and Romania (Delfino et al., 2008). From a phylogenetic point of view, *Allodaposuchus* has been considered for a long time as a sister taxon of the family Hylaeochampsidae (see Buscalioni et al., 2001; Delfino et al., 2008; Puértolas-Pascual, Canudo & Moreno-Azanza, 2013), but also included within Alligatoroidea (Martin, 2010) or more recently treated as a basal crocodylian (Blanco et al., 2014).

In addition, until the discovery of *Allodaposuchus palustris* (Blanco et al., 2014), the features of the postcranial elements of this genus never were studied in detail. The recovery of new cranial and abundant postcranial material ascribed to *Allodaposuchus* from Casa Fabà site (Tremp Basin Southern Pyrenees; Fig. 1), not only sheds light on the anatomical characteristics of this genus, but also provide new clues for its systematic placement and paleobiological treats.

48 **Geological Settings**

49 The Casa Fabà locality is one of the dozens of Late Cretaceous continental fossil sites allocated within
50 the Tremp Basin (Southern Pyrenees, Catalonia; Riera et al. 2009; Dalla-Vecchia et al., 2014).
51 Discovered by Ana María Bravo and Rodrigo Gaete in 2001, the Casa Fabà site is located about 500 m
52 east to the village of Orcau (Pallars Jussà, Catalonia, Spain), in a ravine area known as Les Olives (Fig.
53 1A).

54 At the end of the Cretaceous, the southern Pyrenean region (NE Iberian Peninsula) consisted of an
55 elongated E-W foreland trough connected to the Atlantic Ocean. In this basin, sedimentation occurred
56 in marine settings up to the Campanian-Maastrichtian boundary. Since then, the sedimentary
57 environment gradually evolved to more continental conditions. As a result of an uplift of successive
58 thrust-sheets involved in the formation of the Pyrenean range (Muñoz et al., 1986; Puigdefàbregas et
59 al., 1986), four synclines can now be distinguished from the east to the west: the Vallcebre syncline,
60 the Coll de Nargó syncline and the Tremp and Àger synclines.

61 In the Tremp syncline, uppermost Cretaceous non-marine deposits have received diverse terminology
62 (see Gaete et al. 2009 for a review). In the present study, we refer to the transitional to fully continental
63 materials deposited from the early Maastrichtian to the Thanetian as the Tremp Formation. This
64 formation was divided into four lithologic units by Rosell, Linares & Llompart (2001), which are from
65 the base to the top: 1) a transitional 'grey unit' (marls, coals, limestones, and sandstones), 2) a fluvial
66 'lower red unit' (mudstones, sandstones, oncoids, and paleosols), 3) the lacustrine 'Vallcebre limestone'
67 and laterally equivalent strata and, 4) a fluvial 'upper red unit' (mudstones, sandstones, conglomerates
68 and limestones).

69 Although the Casa Fabà site is mostly covered by abundant vegetation, the outcrop consists on a
70 surface of about 4 m^2 of a sandstone layer with carbonate matrix interbedded between grey marl strata.
71 These sediments are characteristics from the ‘lower red unit’. The occurrence of *Microchara punctata*
72 in those marl deposits would indicate an age of late Maastrichtian according to recent results of
73 Vicente et al. (2015). These authors described a local *Microchara punctata* biozone ranging from the
74 middle part of chron C31r to lower part of chron C30n in the Vallcebre Basin. These results concur
75 with the stratigraphic and magnetostratigraphic data of the site, which indicate and age of early late
76 Maastrichtian, within the C31r chrone (Riera et al., 2009; Vila et al., 2012; Dalla-Vecchia et al., 2014;
77 Fig. 1B).

78

Material and Methods

Material

The recovered material were found in a 2 m^2- area (Fig. 1C) represented by both cranial and postcranial elements (Figs. 2-6). Because no duplication of bones existed, and bones are connected or coherent in size, we consider the specimen as a single individual. The skull is represented by the left premaxilla (MCD4763), a fragment of the right dentary (MCD5134), the right jugal and quadratojugal (MCD5129), most of the skull-table (MCD5139), and a damaged fragment of the jaw (MCD4758a), which preserves one tooth. Postcranial skeleton is also preserved and includes a right scapula (MCD4765), a fragmentary right humerus (MCD4758b), a complete right ulna (MCD4760), a right dorsal rib (MCD5127), a proximal part of an indeterminate rib (MCD4757), an anterior vertebra (MCD5131) and three posterior dorsal vertebrae (MCD5136, MCD4769 and MCD5126).

The holotype of *Allodaposuchus palustris* Blanco et al. 2014, and several extant crocodile skeletons were used as material of comparison, including one specimen of *Crocodylus niloticus* (MZB2003-1423), two of *Alligator mississipiensis* (MZB2006-0613, MZB92-0231) and one *Osteolaemus tetraspis* (MZB2006-0039). In addition, we gathered both cranial and postcranial information from literature about extant and extinct crocodilomorphs: *Crocodylus acutus* (Mook, 1921), *Sebecus icaeorhinus* (Pol et al., 2012), *Allodaposuchus precedens* (Buscalioni et al., 2001, Delfino et al., 2008) and *Allodaposuchus subjuniperus* (Puértolas-Pascual, Canudo & Moreno-Azanza, 2013).

Descriptive anatomy

Osteological descriptions are according to these studies about other species of the genus *Allodaposuchus* (Buscalioni et al., 2001; Delfino et al., 2008; Puértolas-Pascual, Canudo & Moreno-Azanza, 2013; Blanco et al., 2014), and phylogenetical characters (Brochu 2011). In addition, terminology of myological description is according to Meers (2003).

Phylogenetic informed analyses

Phylogenetic relationships of the specimen from Casa Fabà were explored using the dataset of Brochu (2011). However modifications in some operational taxonomic units (OTUs) and characters were carried out (see Supporting Information S1).

The whole dataset resulted in 86 OTUs coded for a total of 181 craniodental and postcranial characters. The taxon *Bernissartia fagesii* Dollo 1883 was used as outgroup. Dataset was analyzed with TNT v1.1

(Willi Hennig Society Edition, (Goloboff et al., 2008). Tree-space was explored using a heuristic search algorithm (traditional search method) with tree-bisection-reconnection branch swapping and 1,000 random addition replicates holding 10 most parsimonious trees for each replicate. All characters were equally weighted and multistate characters were unordered. Bremer supports and bootstrap frequencies (1,000 bootstrap replicates searched) were used to assess the robustness of the nodes.

Inner structural exploration

A Computed Tomography scanner (CT-scan) was used to explore the morphology and the inner structure of the cranial elements. The remains were scanned by a multidetector computer tomography (Sensation 16; Siemens) at Hospital Universitari Mútua de Terrassa (Terrassa, Spain). The material was scanned at 140 kv and 300 mA with and output of 512x512 pixels per slice, with an interstice space of 0.3 mm obtaining a pixel size of 0.586 mm and processed with the Avizo 7.0 software (FEI VSG company). This process enabled to recognize inner characters of cranial nature.

Nomenclatural Acts

The electronic version of this article in Portable Document Format (PDF) will represent a published work according to the International Commission on Zoological Nomenclature (ICZN), and hence the new names contained in the electronic version are effectively published under that Code from the electronic edition alone. This published work and the nomenclatural acts it contains have been registered in ZooBank, the online registration system for the ICZN. The ZooBank LSIDs (Life Science Identifiers) can be resolved and the associated information viewed through any standard web browser by appending the LSID to the prefix "http://zoobank.org/". The LSID for this publication is: [XXXXXXXXXXXXXXXX]. The online version of this work is archived and available from the following digital repositories: PeerJ, PubMed Central and CLOCKSS.

Institutional Abbreviations: **MCD**, Museu de la Conca Dellà, Lleida, Spain; **MZB**, Museu Zoològic de Barcelona, Barcelona, Spain.

Systematic Paleontology

Order CROCODYLIFORMES Hay 1930, (*sensu* Benton & Clark 1988)

Suborder EUSUCHIA Huxley 1875,

Unranked CROCODYLIA Gmelin 1789, (*sensu* Benton & Clark 1988)

Genus *Allodaposuchus* Nopcsa 1928,

Allodaposuchus hulki sp. nov.

urn:lsid:zoobank.org:act: XXXXXXXXXXXXXXXXXXXXXX

(Figs 2-6)

Etimology: *hulki*, from the character of Marvel, Hulk; due to the strong muscle attachments of the bones.

Diagnosis: *Allodaposuchus hulki* shows the following autapomorphies: Quadratojugal does not extend along the infratemporal fenestra. Spine of quadratojugal significantly reduced. Absence of fossa at anteromedial corner of the supratemporal fenestra. No ridge surrounds the *foramen aërum*. No elevation rounds the rim of external naris. Incisive foramen abuts first and second premaxillary teeth. Teeth bear smooth enamel, low-developed mesial and porterior carinae, and absence of longitudinal grooves in lingual side.

In addition, *A. hulki* presents an exclusive combination of the following synapomorphies: External naris opens in anterodorsal direction. Premaxilla is wider than long. Four premaxillary alveoli, being the third the largest. Premaxillary-maxillary suture does not reach the posterior margin of the incisive foramen. Wide and short orbits, without interorbital ridge in the frontal. Quadrate bears two crests in ventral surface for muscle attachment. Capitate process of the laterosphenoid is anteroposteriorly oriented.

Aside of the previous characters, *A. hulki* has the following ambiguous autapomorphies: Anterolateral, anteromedial and olecranon processes of the ulna well developed. Ulnar shaft lateromedially compressed with lateral and medial grooves. Distal condyles of the ulna turned lateroposteriorly, causing a lateral crest in the shaft. We prefer coding all these autapomorphies as ambiguous, due to the absence of postcranial remains in other species of *Allodaposuchus*. New discoveries may reveal if they are autapomorphies of the genus.

Holotype: MCD4763, MCD5129, MCD5139, MCD5134, MCD4765, MCD4757, MCD4758a, MCD4758b, MCD4760, MCD5127, MCD5131, MCD5136, MCD4769 and MCD5126.

Locality, age and horizon: Casa Fabà site, Tremp Basin (NE Spain); lower part of the 'lower red unit' of the Tremp Fm; C31r of the late Maastrichtian (Late Cretaceous).

Description

Cranial skeleton

The cranial remains consist in an isolated left premaxilla (MCD4763), jaw fragments (MCD5134 and MCD4758a), an isolated right jugal and quadratojugal (MCD5129), and a posterior cranial fragment (MCD5139) that preserves frontal, left prefrontal, parietal, both squamosals, postorbitals, exooccipitals, left quadrate and laterosphenoid in connection (Figs. 2, 3). The preserved portion of the skull table is markedly medially concave, with nearly horizontal sides and displays roughly straight margins. The supratemporal fenestrae are filled with sediment (Fig. 2A-B). We estimated a total width ranging from 27 cm (from both lateral hemicondyles of the quatdrates) to 34 cm (from both lateral edges of the quatdratojugals).

Cranial openings

The external naris is undivided and keyhole-shaped (Fig. 3A-B). It is 3.2 cm wide and opens in antero-dorsal direction. In ventral view, there is a small and subcircular incisive foramen (1.7cm wide), which its anterior rim is located, between the first and second alveoli (Fig. 3B). The medial margin of the left orbit is preserved being able to interpret its general morphology. The orbits are relatively wide and short, rounded with their rostromedial margin somewhat elevated. Supratemporal fenestrae are subcircular in shape (4.5cm maximum width) and filled with sediment. There is no fossa around the supratemporal fenestrae. The otic aperture is developed between the squamosal, quadrate and exoccipital, and the cranioquadrate passage forms a caudolaterally open sulcus called *canalis quadratosquamosoexoccipitalis* (Buscalioni et al., 2001; Delfino et al., 2008). The squamosal and the quadrate are not in contact posteriorly to the otic opening.

Premaxilla

It is a nearly complete and not flattened robust bone. Premaxilla is rounded, wider than long. Its posterodorsal margin is slightly eroded, thus presence of a notch or pit in the palatal side of premaxillary-maxillary suture, neither the length of premaxillary process, could not be confirmed. It contacts the maxilla posterolaterally, and probably the nasals medially (Fig. 3A-B). There is no elevation along the lateral and rim of the naris, and neither seems to have it posteriorly. The naris opens flush with the dorsal surface of the premaxilla, without the development of any lateral notch. The internal cavity of the naris shows a large foramen in the rostral-most portion of the left surface,

and several longitudinal ridges caudally to the incisive foramen, probably for soft tissues or muscle attachment. On the palatal surface, the premaxillary-maxillary suture does not abut the posterior margin of the incisive foramen, being completely included within the premaxilla. There are four premaxillary alveoli. Unfortunately, only one tooth root is preserved within respectively alveoli: the first premaxillary alveoli is the smallest, the second and fourth are similar in size, and the third is the largest (Fig. 3B). There is one occlusal pit between the first and second alveoli, and other between the second and third. No pit is present between the third and fourth alveoli.

Jugal

A complete right jugal bone, not preserving the posterorbital bar, has been recovered (Fig. 3D-E). It displays an elongated morphology and shows ornamented external surface. Rostral and caudal edges of the jugal are respectively lateromedial turned, keeping approximately constant lateromedial width. Along the orbit, the jugal dorsal margin is slightly elevated for contact with the lacrimal, making a rounded ventral margin of the orbit. Postorbital bar is lost, but the insertion on the jugal can be defined as 'inset'. In lingual view, an uncommon large medial jugal foramen can be observed rostrally to the postorbital bar insertion. Another smaller foramen is also present rostrally to the former. Ventrally to these foramina, the symphysis with the maxilla begins and continues to the rostral edge.

Quadratojugal

Quadratojugal is a short and wide bone, forming posterior angle of the infratemporal fenestra (Fig. 3D-E). It does not bear any process along lower temporal bar. It also does not extend to superior angle of the infratemporal fenestra. Quadratojugal spine is nearly absent and low in position, near of the posterior angle of infratemporal fenestra. In lateral side, jugal and quadratojugal bear the same ornamentation pattern as the skull table.

Quadrate

Only the left quadrate is complete being part of MCD5139 (Fig. 2). In lateral view, the quadrate contacts the squamosal rostrally, and the exoccipital caudally, forming the anteroventral margin of the external otic aperture and the ventral limit of the cranioquadrate passage. Quadrate also contacts to the postorbital ventrally to the skull table, in the dorsal margin of the infratemporal fenestra. In dorsal view, the quadrate is short caudally to the paroccipital process of the exoccipital bone. Both articular

hemicondyles are similar in size, although the medial hemicondyle is slightly smaller and ventrally deflected (Fig. 2C). From the posteroventral corner of the otic aperture, a soft sulcus passes along the quadratoexoccipital suture, in posterolateral direction, parallel to the cranioquadrate passage, and ends abruptly. The *foramen aërum* is small and located on the dorsal surface, near of the medial edge of the quadrate. Any ridge surrounds the *foramen aërum*. In ventral view, there are two well-marked crests corresponding to the muscle scars A and B of Iordansky (1973), without association of any tubercle (Fig. 2B). In contrast, right quadrate is immediately broken ventrally to the otic aperture, showing the otic canal, also named *cavum tympanicum propium*, filled with sediment.

Frontal

The frontal forms the posteromedial corners of the orbits and the anteromedial corners of the supratemporal fenestrae. It contacts the postorbital laterodorsally and the parietal caudally (Fig. 2A). Frontal prevents contact between postorbital and parietal. The frontoparietal suture is nearly linear and enters the rostromedial margins of the supratemporal fenestrae. The dorsal surface of the frontal is markedly ornamented by subcircular pits that may reach 3 mm in diameter. The main body of the frontal is strongly concave medially, and the orbital margins are upturned. No interorbital ridge is present. The anterior process of the frontal is not preserved. At least part of the left prefrontal is also preserved in MCD5139 (Fig. 2A-B).

Parietal

It contacts the frontal anteriorly and the squamosal laterally (Fig. 2A). There is no contact between the parietal and the postorbital in dorsal view. The parietosquamosal suture enters the supratemporal fenestra caudally. Contact with the supraoccipital could not be assessed due to preservational reasons. The parietal is longer than wide and displays a marked ornamentation in dorsal surface, consisting in the same subcircular depressions present in the rest of the skull bones. The parietal is medially concave, as part of the general concavity of the skull table. A recess in the parietal communicates with the pneumatic system.

Postorbital

It contacts the squamosal posteriorly and the frontal anteromedially. In MCD5139, both postorbitals are longer than wide, displaying a well-curved contour in dorsal view (Fig. 2A). Postorbital constitutes

the anterolateral corner of the supratemporal fenestra, conferring rounded anterior edges to skull table. It also forms posterior orbital margin and the anterodorsal corner of the infratemporal fenestra. The ornamentation is the same as the rest of the skull table.

Squamosal

Squamosal is a triangular-shaped bone which contacts the postorbital anteriorly, the parietal medially, the quadrate anteroventrally, and the exoccipital posteroventraly, constituting the cranioquadrate passage (Fig. 2D). Posteriorly to the passage, the quadrate and the squamosal are separated by the exoccipital. In lateral view, two rims delimited a longitudinal groove for external ear valve musculature. These dorsal and ventral rims are parallel. In dorsal view, the suture between the squamosal and the postorbital is very posteriorly situated, reaching the caudal-most part of the lateral margin of the supraorbital fenestra. Squamosal develops a significantly posterolateral extension conforming a horizontal the margin of the skull table. In occipital view, the squamosal slopes ventrolaterally over the exoccipital, but squamosal does not laterally surpass the paroccipital process of the exoccipital.

Supraoccipital

Skull table is damaged coinciding with the supraoccipital location, thus morphology of the supraoccipital and its relationships with the other bones could not be assessed with confidence.

Exoccipital

It occupies most of the occipital surface, contacting the squamosal dorsally, and quadrate lateroventrally (Fig. 2). Exoccipital conforms the caudoventral margin of the cranioquadrate passage. Paroccipital process does not extend much laterally, ending in the medial quadrate branch. In occipital view, exoccipital shows a very prominent boss on paraoccipital process. The foramen magnum is relatively preserved, but the ventral edges of exoccipitals are broken, and suture with the basioccipital is missing.

Laterosphenoid

In palatal view, laterosphenoid is situated medially in the braincase, between the supratemporal fenestrae (Fig. 2B). It contacts frontal rostrally and postorbitals laterally, conforming rostromedial

295 marging of supratemporal fenestra in ventral view. The capitate process of the laterosphenoid is
296 anteroposteriorly oriented.
297
298 **Dentary**
299 Only a right fragment of the anterior part of the dentary was recovered (MCD5134), which is very
300 fragmentary and incomplete (Fig. 3C). According to the medial curvature of the bone, we have
301 interpreted it as the rostral-most portion of the right dentary, bearing from the first to fourth alveoli.
302 Lingual surface of the bone is not preserved, showing the alveoli in section. Only two teeth are
303 preserved in situ, the second and the fourth, projecting anterodorsally. In the second alveolus, the
304 functional tooth is lost, but there is a replacement non-erupted tooth. In contrast, the fourth tooth is a
305 caniniform.
306 MCD4758a is an indeterminate fragment of the jaw. Due to preservation reasons, it is not possible to
307 elucidate side or position that belongs within the jaw. This fragment preserves three alveoli, bearing
308 one erupted tooth (Fig. 3F-G).
309
310 **Dentition**
311 Teeth are circular in section. Tooth crown are slightly blunt. Enamel lacks ornamentation, but several
312 longitudinal ridges appear in the most basal portion of the crown in lingual side. Anterior and posterior
313 keels are low developed, and there are not longitudinal grooves next to the keels in lingual side. These
314 ridges are soft in MCD4758a, and more developed in the caniniform tooth of MCD5134. Replacement
315 tooth of MCD5134 lacks ridges, probably due to be a non-erupted tooth (Fig. 3C)
316
317 **Postcranial skeleton**
318 Recovered postcranial skeleton of *Allodaposuchus hulki* is composed by a distal end of the right
319 scapula (MCD4765), right humerus (MCD4758b), right ulna (MCD4760), two dorsal ribs (MCD4757
320 and MCD5127) and five vertebrae (one dorsal, three lumbar, and fragments of an indeterminate one,
321 MCD5131, MCD5136, MCD4769, MCD5126 and MCD5125, respectively).
322
323 **Scapula**
324 Only the ventral edge of the scapula is preserved, showing the glenoid fossa, the deltoid crest, the
325 anterior process of the scapula and the part of the scapular blade (Fig. 4A-D). The scapular blade is

constricted at its beginning, and seems to flare dorsally. In posterior view, the scapular blade is sinuous. The glenoid is oriented posterolaterally. In lateral view, the posterior end of scapular blade is straight. Lateral surface of the scapula bears several rugose areas (Fig. 4A). A rugose zone for the insertion of the *M. serratus ventralis thoracis* (Meers, 2003) is situated in the posterior edge of the scapular blade. In the same side, but in a most ventrally position where the blade is constricted, other rugose area evidences the origins of the *M. scapulohumeralis caudalis,* and immediately superior to supraglenoid buttress a highly-developed rugosity constitutes the origin of the *M. triceps longus lateralis* (Meers, 2003). The anterior process of the scapula bears a wide deltoid crest. This crest is the origin of the *M. coracobrachialis brevis dorsalis* and the *M. deltoideus clavicularis*. Ventrally to the deltoid crest, a more soft rugose area evidences the origin of the *M. supracoracoideus intermedius* (Fig. 5A-C; Meers, 2003). In medial view, the scapula also shows several rugose areas for muscle attachment (Fig. 4A). The medial surface of the blade shows the origin of *M. subscapularis,* and *M. triceps longus caudalis* (Fig. 5A; Meers, 2003). In this view, a small foramen is present at the base of the scapular blade. The anterior process of the scapula also bears a soft rugose area for the origin of *M. supracoracoideus longus* (Meers, 2003). In ventral side, the scapula-coracoid facet is present, and is broader caudally (Fig. 4D). Coracoid is not fused to the scapula. The sutural surface is teardrop-shaped, and the lateromedial width in the posterior portion is much greater than the anterior one.

Humerus

A right humeral diaphysis was recovered (Fig. 4E-H). The proximal articular surface is eroded. The anterior tuberosity and the humeral head seem to have the same high, and the posterior tuberosity seems to be slightly distally positioned. The deltopectoral crest is lost. In lateral view, the proximal portion of the shaft is dorsally concave, and its distal portion is ventrally turned. The lateral surface of the humerus is slightly concave. In turn, the medial surface of the humerus is slightly convex. The shaft is broken before the distal condyles.

Like scapula, the humerus also shows several rugous areas around itself. In posterior view (Fig. 4G), a wide rugous area is situated caudally to the condyles, corresponding to the insertion of the *M. scapulohumeralis caudalis* (Fig. 5D-G; Meers, 2003). The dorsal surface bears a single insertion scar for *M. teres major* and *M. dorsalis scapulae* (according to Brochu, 2011), or *M. teres major* and *M. latissimus dorsi* (according to Meers, 2003). The shaft shows small and soft ridges occupying completely the dorsal surface. These ridges correspond at least to the origin of the *M. triceps brevis*

intermedius, and possibly of the *M. triceps brevis cranialis* (Meers, 2003), but limits between both muscles are not distinguished. The origins of *M. triceps brevis intermedius*, extends to medial side of the shaft (Fig. 5D-G). The lateral surface of the shaft shows part of the origins of *M. triceps brevis intermedius*, and the origin of the *M. humeroradialis* (Meers, 2003). Deltopectoral crest is lost, lacking most of the *M. deltoideus clavicularis* insertion (Meers, 2003). A small crest (lineae intermuscularis humeroradialis-brachialis) is situated laterally to the insertion of *M. teres major*. In ventral view (Fig. 5D-G), descriptions for muscle attachment in the proximal epiphysis could not be made due to preservational reasons. However, the shaft shows the end of the origin of *M. triceps brevis intermedius* in medial margin, and the end of the origin of *M. humeroradialis* in the lateral one. At the middle of the shaft the origin of *M. brachialis* is present (Meers, 2003), distally to the deltopectoral crest location.

Ulna

The right ulna is one of the best-preserved bones (Fig. 4H-K). The proximal end of the ulna is anterioposteriorly expanded. In proximal view is triangular-shaped, with very prominent vertex. The olecranon process is acute, and the articular surface for the radius is concave. There is a very sharp process medially to the articular surface for the radius. The shaft is comprised mediolaterally, and shallow grooves could be discerned in medial and lateral sides. The distal half of the shaft is prominently oriented anteriorly. Both distal condyles are compressed and anterolateral to mediocaudally oriented. As result of this torsion, there is a ridge in the lateral side of the distal end of the ulna.

The ulna also shows several muscle attachments. A rugosity abuts the olecranon process in caudal, lateral and medial views, and evidences the insertion of *M. triceps brachi* (Meers, 2003). In lateral view (Fig. 4H), the *M. flexor ulnaris* origins in a groove situated immediately distally to the sharp process of the articular surface of the radius. *M. flexor ulnaris* disposes over the lateral ridge of the ulna. Rostrally to it, a very soft ridge conforms de origin of *M. extensor carpi radialis brevis – pars ulnaris*, near of the anterior margin and facing to the radius (Fig. 5H). In medial side (Fig. 4I), other groove supports the origin of *M. pronator quadratus* (Meers, 2003). A small crest situated caudally to this groove, in addition to other soft ridges comprise the origin of *M. flexor digitorium longus* (Fig. 5I; Meers, 2003). There also are very rough areas laterally and medially to the distal condyles for ligaments attachments, being the lateral one more developed than the medial.

388 **Vertebrae**

389 The preserved vertebrae have been sorted based on the presence of the keels and the position of the
390 parapophyses, according to Mook (1921). The fourth dorsal vertebrae (MCD5131) and the first
391 (MCD5136), second (MCD4769) and third (MCD5126) lumbar have been recovered. All vertebrae are
392 strongly procoelus.

393 MCD5131 (Fig. 6A-D) is broken laterally, and prezygapophyses, right diapophysis and parapophysis,
394 and neural spine are lost. Postzygapophyses are elongated lateromedially and short anteroposteriorly,
395 its articular surface faces ventrally and is lateromedially inclined. The left parapophysis is located at
396 the base of diapophysis. The diapophysis is elongated and dorsolaterally oriented, but thin
397 anteroposteriorly. The centrum and the neural arch are completely fused. The centrum is relatively
398 short anteroposteriorly. A well-developed hypapophyseal keel is present ventrally to the centrum. Wide
399 striated areas can be observed at the base of neural arch, under the diapophyses and postzygapophyses,
400 in the ventral side of the centrum, and dorsally to the neural arch, between the diapophysis, post- and
401 prezygapophysis, and neural spine. These areas are consistent with a strong muscle attachment.

402 Lumbar vertebrae (MCD5136, MCD4769 and MCD5126; Fig. 6E-P) are partially broken or eroded.
403 Pre- and postzygapophyses are broader than those of the dorsal, and progressively wider from first to
404 third lumbar. Neural spines are partially broken, but they seem to be wide anteroposteriorly and low.
405 Transverse processes are horizontally oriented, and progressively decrease in high respect the centrum.
406 They are laterally shorter and anteroposteriorly wider from first to third lumbar. There is a longitudinal
407 groove ventrally to the centrum in all lumbar vertebrae. Like the dorsal vertebrae, wide striated areas
408 are present laterally to the neural arch, across the diapophyses, in the ventral side of the centrum, and
409 between the diapophysis, post- and prezygapophysis, and neural spine. These areas are consistent with
410 a strong muscle attachment.

411

412 **Ribs**

413 Two partial ribs have been recovered. One of them comprises only the shaft of a right dorsal rib
414 (MCD5127) lacking its capitular and tubercular processes. It is elongated (19.2 cm long) and
415 lateromedially comprised. In section, it is teardrop-shaped, with its thinner margin cranially, forming
416 an anterior crest of the shaft. Soft ridges for muscle or ligaments attachments are present lateral and
417 medially in the distal-most portion of the shaft. In turn, MCD4757 consists in the capitular and
418 tubercular processes of an anterior-most left dorsal rib, which lacks the shaft.

419

420 **Comparative Anatomy**

421 Cranial remains are comparable to other species of *Allodaposuchus,* especially to the nearly complete
422 skulls of *A. precedens* and *A. subjuniperus* (Delfino et al., 2008 and Puértolas-Pascual, Canudo &
423 Moreno-Azanza, 2013; respectively). However, postcranial remains are only comparable to *A. palustris*
424 (Blanco et al., 2014) due to absence of published material of the others.

425 Several characters of the premaxilla distinguish *Allodaposuchus hulki* from the other species of the
426 genus. The external naris opens in antero-dorsal direction like *A. precedens*. In turn, naris of *A.*
427 *subjuniperus* opens in dorsal direction. Unlike *A. precedens* and *A. subjuniperus*, there is no elevation
428 along the rim of the external naris. However, no lateral notch develops on dorsal surface of premaxilla
429 next to the naris opening, like *A. precedens* and *A. subjuniperus*. In palatal view, the incisive foramen
430 is located more anteriorly than *A. precedens* and *A. subjuniperus*. In *A. hulki* the anterior rim of incisive
431 foramen is located between the first and second alveoli, whereas in *A. precedens* and *A. subjuniperus*,
432 reaches the third premaxillary alveolus. Premaxilla is wider than long, like *A. subjuniperus.* However,
433 like *A. precedens,* the premaxillary-maxillary suture does not reach the posterior margin of the incisive
434 foramen. The number of premaxillary alveoli is four, being the third alveolus the largest, like *A.*
435 *subjuniperus.* The premaxilla of *A. precedens* shows five teeth and the fourth is the largest. Moreover,
436 *A. hulki* shows a pattern of oclusal pits different to *A. precedens* and *A. subjuniperus*.

437 In addition, the skull table of *A. hulki* also shows differences from the other species of the genus. The
438 main body of the frontal is concave medially, like *A. palustris* and *A. precedens*, and the orbital
439 margins are upturned. However, this concavity is strongly marked in *A. hulki*, but slightly in *A.*
440 *palustris* and *A. precedens*. In turn, *A. subjuniperus* shows a practically flat frontal with a low
441 transverse interorbital ridge at the beginning of the anterior process. *Allodaposuchus palustris* also
442 shows the interorbital ridge. Nevertheless, no interorbital ridge is present in *A. hulki* and *A. precedens*.
443 The orbits of *A. hulki* are wide and short, like *A. precedens* and *A. subjuniperus.* In turn, *A. palustris*
444 shows relatively large and elongated orbits. However, the four species of *Allodaposuchus* have an
445 elevated rostromedial margin of the orbits.

446 The frontoparietal suture of *A. hulki* is nearly linear, like *A. subjuniperus* and *A. precedens*.
447 *Allodaposuchus palustris* is the only 'allodaposuchian' that shows a concavo-convex frontoparietal
448 suture. Additionally, *A. hulki* and *A. palustris* are the two species that do not show a fossa around the
449 supratemporal fenestrae.

Like *A. precedens*, both articular hemicondyles of the quadrate of *A. hulki* are similar in size, although the medial hemicondyle is slightly smaller and ventrally deflected. In turn, *A. subjuniperus* shows a ventral expansion in the medial hemicondyle. The *foramen aërum* of *A. hulki* is small, like *A. precedens* and *A. subjuniperus*, but large in *A. palustris*. This foramen is located on the dorsal surface, near of the medial edge of the quadrate, in all the species of *Allodaposuchus*. However, in *A. hulki* no ridge surrounds the *foramen aërum*, unlike the other three species of *Allodaposuchus*. Like *A. subjuniperus*, in ventral view there are the two muscle scars of Iordansky (1973), without association of any tubercle. *Allodaposuchus precedens* only shows one crest ending abruptly and forming a small tubercle, and *A. palustris* does not show any crest.

The exoccipital of *A. hulki*, *A. subjuniperus*, and *A. precedens* bears a very prominent boss on the paraoccipital process. *Allodaposuchus palustris* is the only 'allodaposuchian' that does not show this boss.

In ventral view, the capitate process of the laterosphenoid is anteroposteriorly oriented in *A. hulki* and *A. subjuniperus*, but is laterally oriented in *A. precedens*.

The quadratojugal of *A. hulki* shows a characteristic shape that represents a few autapomorphies of this taxon. Unlike *A. precedens* and *A. subjuniperus*, quadratojugal does not extend to superior angle of infratemporal fenestra. Moreover, quadratojugal spine is almost absent and near of the ventral angle in the fenestra infratemporal. *Allodaposuchus precedens* and *A. subjuniperus* show the quadratojugal spine in a higher position in the fenestra. This spine is highly developed in *A. subjuniperus*.

The dentition of *A. hulki* also shows several characters that distinguish itself from the other species of the genus. In *A. hulki*, the enamel lacks ornamentation, both anterior and posterior carinae are poorly developed, and there are not longitudinal grooves in lingual side. In contrast, *A. palustris* and *A. precedens* show ornamented enamel with well-developed carinae, whereas *A. subjuniperus* and *A. palustris* bear well-marked longitudinal grooves in lingual side.

Concerning axial skeleton, all recovered vertebrae are procoelous. This character clearly indicates a eusuchian condition (Salisbury et al., 2006). Preserved dorsal and lumbar vertebrae are similar in shape to those of *Crocodylus acutus, Crocodylus niloticus*, *Alligator mississipiensis* and *Osteolaemus tetraspis* and *Allodaposuchus palustris*. However, all the vertebrae of *A. hulki* show wide areas for muscle or ligament attachment, absent in those of *A. palustris*.

The appendicular skeleton is poorly comparable to *A. palustris*, due to the former does not preserve scapula and ulna, but a fragmentary humerus, radius and hindlimb bones (Blanco et al., 2014). The

scapula of *A. hulki* is similar in shape to those of extant crocodylians. The scapular blade shows a constriction immediately dorsally to the glenoid and anterior process, and flares dorsally. However, in caudal view, the glenoid is more conspicuous and the scapular blade is more sinuous than in extant taxa. In addition, scapula of *A. hulki* bears more developed scars for the origin of *M. scapulohumeralis caudalis, M. triceps longus lateralis, M. supracoracoideus intermedius* and *M. supracoracoideus longus* than in other compared taxa. The humerus of *A. hulki* is clearly more robust and also shows more developed origins of *M. humeroradialis* and *M. brachialis* than in *A. palustris* and other extant taxa. In the latest taxa, the humeral surface is mainly smooth, but in *A. hulki* is completely covered by soft ridges for muscle attachments. However, the humerus of *A. hulki* resembles those of compared taxa in shape. In contrast, the ulna of *A. hulki* largely differs from the morphology of the extant crocodylians. The proximal epiphysis of the ulna of *A. hulki* has three well-developed processes (the olecranon directed posteriorly, an anteromedial process, and an anterolateral process). These processes are weakly developed in extant crocodylians, but well-developed in *Sebecus* and other terrestrial notosuchians (Pol et al., 2012; and references therein), despite the general morphology of the proximal surface of the ulna of *Allodaposuchus* does not resemble these taxa. The shaft of this bone is lateromedially compressed in *A. hulki*, unlike the other compared taxa that show a subcircular shaft in cross section. Additionally, the torsion of the distal condyles, the crest for the origin of *M. flexor digitorium longus,* and the lateral and medial grooves for the origin of *M. flexor ulnaris* and *M. pronator quadratus*, respectively, have not been seen in other taxa used for comparison.

Thus, given all discussed above, *Allodaposuchus hulki* seems to be morphologically intermediate to *A. subjuniperus* and *A. precedens*, with several unique characters. In addition, as noted by Blanco et al. (2014), the appendicular skeleton seems to be conservative in fossil and living taxa. Nevertheless, despite appendicular bones could not be directly compared between *A. hulki* and *A. palustris*, both 'allodaposuchians' show stronger muscle and ligament scars than in other taxa used for comparison.

Results

Endocranial configuration

As typical for archosaurs the brain did not occupy the entire endocranial cavity. The 3D reconstruction of the cranial fragment reveals the morphology of some parts of the olfactory bulbs, the cerebral hemispheres, cranial nerves, inner middle ear and tympanic recesses (Fig. 7).

The preserved portion of the endocast shows the typical sigmoid morphology. However, just the most anterior part of the olfactory bulbs are preserved while the cerebral hemisphere is dorsally well preserved but lacking some ventral areas due to preservation reasons. Some of the left side cranial nerves are recognizable, in particular the nerve V system, particularly the V_1, V_2 and V_3 as well as nerves III, IV and XII. The inner middle ear is present but badly preserved. Moreover, the low pixel resolution of the CT scan avoids to assessing with confidence its morphology and it is not included in the figures (Fig. 7E).

Of particular interest are the tympanic recesses in the cranial fragment. On one hand, the intertympanic recess is very developed. In extant crocodiles, as *Crocodylus johnstoni* (Witmer et al. 2008), the anterior part of the intertympanic recess present a semicircular morphology, while in the described specimen, a complete circle morphology is found due to the development of an anterior portion. In connection with the intertympanic recess there is the *cavum tympanicum propium* with similar morphology as in other extant crocodiles. But, on the other hand, the quadrate sinus is very wide in comparison with other extant crocodiles (Witmer et al. 2008; Witmer & Ridgely 2008) in the reported specimen.

Phylogenetic relationships

The cladistic analysis resulted in 1240 equally parsimonious cladograms of 600 steps (CI = 0.382; RI = 0.811; RC = 0.310), and includes the specimen from Casa Fabà in the genus *Allodaposuchus*. The strict consensus tree (Fig. 8) shows similar topology than the last hypothesis about *Allodaposuchus* emplacement (Blanco et al., 2014), in contrast to some previous works that suggest *Allodaposuchus* as sister taxa of hylaeochampsids (Buscalioni et al., 2001, Delfino et al., 2008, Puértolas-Pascual, Canudo & Moreno-Azanza, 2013) or derived alligatoroid (Martin, 2010). In the present analysis, as in Blanco et al. (2014), the clade 'Allodaposuchia' was included within Crocodylia, placed in a more derived position than Gavialoidea, and forming a polytomy with *Borealosuchus*, Planocraniidae and the clade Brevirostres (Crocodyloidea + Alligatoroidea). However, in the present analysis the relationships between *Arenysuchus* and *Allodaposuchus* species were better resolved. In Blanco et al. (2014), *A. palustris* is the most basal 'allodaposuchian', whereas *A. precedens*, *A. subjuniperus,* and *Arenysuchus* form a polytomy. Our results suggest that *A. precedens* and the eusuchian from Casa Fabà are more derived than *A. subjuniperus* and *Arenysuchus.* Both results agreed that *A. palustris* is the most basal crocodylian of the genus, and that *Arenysuchus gascabadiolorum* could be included within the Genus

Allodaposuchus. However, the inclusion of *Arenysuchus* in this genus exceeds the aim of this paper, and should be revised in detail in future works.

Discussion

Phylogeny

The most parsimonious hypothesis obtained in our analyses suggests that the clade 'Allodaposuchia' belongs to Crocodylia (Fig. 8). Even though the Bremer and bootstrap values were low, the clade 'Allodaposuchia' has similar support than other clades of Crocodylia. According to Blanco et al (2014), the genus *Allodaposuchus* might represent more derived eusuchian crocodylomorph than previously thought (Buscalioni et al., 2001, Delfino et al., 2008, Puértolas et al., 2013, Narváez & Ortega 2011) but not as derived as in Martin (2010). This hypothesis is supported by several cranial and vertebral characters. According to Brochu (1997), the inclusion of the clade 'Allodaposuchia' within Crocodylia would be supported by the following synapomorphies: 1) anterior dentary teeth project anterodorsally, 2) retroarticular process projects posterodorsally, 3) frontoparietal suture concavo-convex, 4) mature skull table with nearly horizontal sides, and long posterolateral squamosal rami along paraoccipital process, 5) exoccipital lacks boss on paraoccipital process, and 6) hypapophyseal keels are present on the eleventh vertebrae behind the atlas. Absence of the boss in paraoccipital process, only in *A. palustris*, would be an ancestral state reverted in the other members of the clade 'Allodaposuchia' (Blanco et al., 2014). The following synapomorphies related *Allodaposuchus* with *Borealosuchus* + Planocraniidae + Brevirostres (*sensu* Brochu (1997)): 1) slender postorbital bar, 2) ventral margin of postorbital bar inset from lateral jugal surface, 3) skull table surface planar at maturity, 4) frontoparietal suture concavo-convex, 5) neural arch of the axis lacking lateral processes (diapophyses), 6) wide posterior half of the axis neural spine, 7) axial hypapophysys without deep fork, 8) M. *teres major* and M. *dorsalis scapulae* inset with common tendon on humerus. The concavo-convex frontoparietal suture, only in *A. palustris*, would be a reverted state in the other members of the clade 'Allodaposuchia' (Blanco et al., 2014).

The inclusion of the Casa Fabà eusuchian within genus *Allodaposuchus* is well supported by the phylogenetic analyses (Fig. 8) and qualitative data (see above). *Allodaposuchus* differs from all other eusuchians by the exclusive combination of the following synapomorphies (Blanco et al., 2014): margin of the orbits upturned; quadrate and squamosal not in contact on the external surface of the skull, posteriorly to the external auditory meatus; caudal margin of otic aperture not defined and

gradually merging into the exoccipital; dermal bones roof overhang rim of supretemporal fenestra; cranioquadrate passage or canalis quadratosquamosoexoccipitalis laterally open and represented by a sulcus (broader than in *Hylaeochampsa vectiana*), with the exoccipital between the squamosal and the quadrate posterior to otic aperture. Ventral process of the exoccipital not involved in the basioccipital tubera; quadrate *foramen aërum* on dorsal surface. When preserved, all the characters found in the specimen of Casa Fabà are in agreement with the synapomorphies of *Allodaposuchus*.

Allodaposuchus hulki, A. precedens and *A. subjuniperus* share a linear frontoparietal suture, the presence of a shallow fossa at anteromedial corner of supratemporal fenestra (posteriorly reverted in *Allodaposuchus hulki*), and the exoccipital with very prominent boss on paraoccipital process.

Allodaposuchus hulki, and *A. precedens* share the incisive foramen abutting premaxillary tooth row, and a very large medial jugal foramen. Such foramen is larger in *A. hulki* than in *A. precedens*, and consequently than in any other *Allodaposuchus*.

Allodaposuchus hulki shows some autapomorphies compared to other members of the clade 'Allodaposuchia': quadratojugal that does not extend along the infratemporal fenestra, absence of fossa at anteromedial corner of supratemporal fenestra, and teeth with characteristic morphology. In contrast, *A. precedens* shows dermal bones of skull roof not overhanging supratemporal fenestra rim, and capitate processes of laterosphenoid laterally oriented. All these differences justify the assignment of the specimen from Casa Fabà to a different species within *Allodaposuchus*.

In addition to the characters provided in the phylogenetical matrix, several qualitative morphological characters could be added to the phylogenetic results (see above). *Allodaposuchus hulki* shows several unique characters unlike other species of *Allodaposuchus*: there is no elevation around the rim of external naris, incisive foramen located between the first and second alveoli, quadratojugal spine nearly absent, and located near of the ventral angle in the infratemporal fenestra, no ridge surrounds the *foramen aërum*, and teeth with smooth enamel, low-developed carinae, and absence of longitudinal grooves in lingual side, showing a occlusal pattern in the premaxilla different to the other 'allodaposuchians'. *Allodaposuchus hulki* and *A. precedens* also share the following characters: external naris opened in aterodorsal direction, premaxillary-maxillary suture does not reach the incisive foramen, absence of interorbital ridge and medial articular hemicondyle of the quadrate ventrally deflected. Finally, a few characters shared between *A. hulki* and *A.subjuniperus* could be considered as ancestral condition, and posteriorly derived in *A. precedens*: premaxilla wider than long with four teeth

positions, being the third the largest, two crests in the ventral surface of the quadrate without association of any tubercle, and capitate processes of laterosphenoid anteroposteriorly oriented.

As previously discussed, *Allodaposuchus hulki* seems to be morphologically intermediate to *A. subjuniperus* and *A. precedens*, with several unique characters that justify the assignment of this specimen to a different species.

Cranial pneumaticity and paratympanic recesses

On recent times, the virtual reconstruction of cranial cavities of extant and extinct archosaurs has provided an enormous advance on the knowledge about the configuration and evolution of the brain regions and the surrounding bony recesses. Most of these studies focus on the endocast morphology as well as the inner ear disposition and its paleobiological implications (e.g. Witmer & Ridgely, 2009; Kley et al., 2010; Fernández et al., 2011; Bona, Degrange & Fernández, 2013, and references therein).

Despite of lacking most of its ventral and posterior-most parts, the general shape of the cranial endocast of *Allodaposuchus hulki* (Fig. 7) is similar to those of extant crocodilians (e.g. *Gavialis gangeticus* Wharton, 2000; *Crocodylus johnstoni*, Witmer et al., 2008; *Alligator mississipiensis*, Witmer & Ridgely 2009; George and Holliday, 2013). Further, the overall configuration of the cranial endocast of the specimen resembles that of many other crocodilomorphs such as notosuchians (e.g. *Anatosuchus* and *Araripesuchus*, Sereno & Larson, 2009; *Simosuchus*, Kley et al., 2010) and metriorhynchids (Fernández et al., 2011). The curvilinear dorsal counter of the endocast exhibited by *Allodaposuchus hulki* is more similar to those observed in Neosuchia (Witmer & Ridgely 2008; George & Holliday, 2013; Fig. 7A) than the characteristic spade-shape outline showed by notosuchians (Sereno & Larson, 2009; Kley et al., 2010). In sagittal view, the shape of the cranial cavity indicates that most of braincase elements were arranged in a planar configuration (Fig. 7D, E), in contrast to the sigmoidal organization of most of extant crocodylians (Witmer et al., 2008; Witmer & Ridgely 2009; George & Holliday, 2013). Another significant feature of the braincase of *Allodaposuchus hulki* is that in dorsal view the cerebrum exhibits a rhomboidal shape, more elongated rostrally than extant crocodiles, and showing a gentle transition to the olfactory track (Fig. 7A, B).

In comparison to the works analyzing braincase morphology, there are few studies focusing in the system of pneumatic cavities surrounding the main endocranial body (Witmer el al., 2008; Witmer & Ridgely, 2009, 2010; Bona, Degrange & Fernández, 2013). In extant crocodiles, the paratympanic system is divided in the three main parts: 1) two caudal tympanic recesses connected by 2) the inner

tympanic recess, which also links 3) the dorsal tympanic recesses located at each side of the endocranial cast (Witmer et al. 2008). The same configuration is observed in the Miocene caimanine *Mourasuchus nativus* (Bona, Degrange & Fernández 2013). Dufeau & Witmer (2007) noted several ontogenetical changes in the tympanic cavities along the life history of *Alligator mississippiensis*. The authors stated that these changes could also be phylogenetically tracked within the crurotarsia linage, as such as that basal taxa show the young alligator condition whereas more crownward taxa resemble the adult one. In this regard, *A. hukli* shows endocranial features of both juvenile (i.e. large quadrate sinuses) and adult alligators (i.e. well-developed dorsal tympanic recesses).

In addition, *Allodaposuchus hulki* exhibits some important differences in the tympanic system configuration observed in extant adult crocodiles. First, it shows a well-developed pneumatic cavity connecting anteriorly both dorsal tympanic recesses. This sinus, herein referred as anterodorsal tympanic recess, covers part of the sphenoparietal dural venous sinus but leaving a circular opening at the level of the occipital dural venous sinus (Fig. 7A). In some ways, it resembles the frontal recess observed in the *Struthio camelus* (Witmer & Ridgely, 2009), but not so developed in *Allodaposuchus*. Although variations in the paratympanic system are reported in more derived archosaurs (i.e. some non-avian theropods exhibit supraoccipital pneumatic sinus connected to the tympanic pneumaticity, and birds have enlarged both dorsal and caudal tympanic recesses; Witmer & Ridgely, 2009; 2010), nothing like the anterodorsal tympanic recess of *A. hulki* is recognized so far. In addition, another distinctive feature of the tympanic system of the new species is the caudolateral expansion of the caudal tympanic recesses; which excavate a large cavity within the exooccipital bones. Such caudal tympanic sinus configuration is not present in any extant crocodilomorph, neither reported previously from any extinct one, but it resembles to that of large non-avian theropods (Witmer et al., 2008; Witmer & Ridgely, 2009; 2010).

The external ear of the genus *Allodaposuchus* is distinguished by a broad cranioquadrate passage, a feature shared with the basal eusuchid *Hylaeochampsa* (Buscalioni et al., 2001; Delfino et al., 2008; Puértolas-Pascual, Canudo & Moreno-Azanza, 2013; Blanco et al., 2014). Although its external morphology has been described in detail by several authors, here we provide the first tridimensional reconstruction of this cranial cavity and its relationship with the tympanic sinus and the braincase (Fig 7). The cranioquadrate passage of *Allodaposuchus hulki* opens to a well-developed *cavum tympanicum proprium* lateromedially directed (Fig. 7A), which connects to the tympanic complex at the level of the dorsal tympanic recesses. In *Crocodrylus johnstoni* the *cavum tympanicum proprium* is more

665 medioventrally directed (Witmer et al., 2008), a condition also noted in the caimaninid *Mourasuchus*
666 (Bona, Degrange & Fernández, 2013). It is worthy to comment that the *cavum tympanicum proprium*
667 of *Allodaposuchus hulki* is ventrally connected to a large quadratic sinus (Fig. 7C).
668 In fact, the large size of the quadratic sinus is another highlighted feature of *Allodaposuchus*. In
669 *Crocodylus johnstoni*, the quadratic sinus is also located above the *cavum tympanicum proprium* but it
670 is smaller than that of the *A. hulki* and extends posterodorsaly to the pharingotympanic recess (Witmer
671 et al., 2008). A long and thin siphonial tube (see Witmer et al., 2008: Fig.6.6.A-B) runs along the
672 quadrate connecting the quadratic sinus and the *siphonimu*. The later connects with the articular recess
673 of the mandible. The siphonial tube is not observed in *A. hulki*, but the place where it was supposed to
674 be is partially occupied by the enlarged quadratic sinus. Thus, we hypothesize that it could be relatively
675 short, extending from the caudal end of the quadratic sinus and the *foramen aërum* placed near the
676 posterior edge of the quadratic hemicondyle.
677 The unique cranial pneumaticity configuration observed in *A. hulki*, especially in regards to the
678 paratympanic system (e.g. an anterodorsal tympanic recess and enlarged caudal tympanic recesses) and
679 the enlargement quadratic sinus, suggests some degree of otic specialization. Although being just a
680 hypothesis, the paratympanic configuration of *A. hulki* could result in more efficient pressure
681 difference receiver mechanism, which is related to directional hearing (Bierman et al., 2014). We hope
682 that future studies could shed light on this question.
683
684 **Forelimb myology and functional morphology**
685 Three types of limb posture are traditionally identified in quadrupedal tetrapods during terrestrial
686 locomotion: sprawling, semi-erected, and erected. Extant crocodiles locomotion ranges from sprawling,
687 in which the limbs are positioned laterally, to semi-erected high walk, in with limbs are strongly
688 adducted (Briknam, 1980; Parish, 1986, 1987; Gatesy, 1991; Allen et al., 2014), while some extinct
689 crocodilomorphs, such as notosuchians, could exhibit the erected posture (Sertch & Groenke, 2011;
690 Chamero, Buscalioni & Marugán-Lobón, 2013; and references therein). However, most of these
691 postures and locomotion inferences are based in anatomical features of the pelvic girdle and hind limbs
692 rather than the pectoral girdle and forelimbs. In addition, the reconstruction of appendicular
693 musculature is also regarded as being increasingly important in understanding locomotion behavior in
694 fossil vertebrates. Thus, recognizing the morphological features in anterior limbs that characterize each
695 type of limb posture is clue to infer not only locomotion but also the lifestyle of *Allodaposuchus hulki*.

From a morphological point of view, the scapula of *A. hulki* exhibits a robust appearance. It is primarily characterized by having a well-developed anterior process with a wide deltoid crest, a marked scapular butter, and scapular blade margins flared dorsally. Although no quantitative analyses can be conducted because the fragmentary nature of the element, the combination of those features is consistent with the general scapular configuration of extant alligatorids and gavialids according to Brochu (1997) and Chamero, Buscalioni & Marugán-Lobón (2013), whereas crocodiles tend to show more slender scapulae with narrow blades. The presence of prominent scapular buttress has been considered characteristic of upright posture in several terrestrial crocodilomorph taxa, while the absence of this treat is characteristic of primarily aquatic ones (Sertch & Groenke, 2011; Chamero, Buscalioni & Marugán-Lobón, 2013). Although the presence of this feature in *Allodaposuchus hulki*, it is not as developed as in terrestrial mesoeucrocodylian (e.g. *Simosuchus* or *Araripesuchus*). Thus, it may indicate some degree of upright posture, but not full erected, or additional bracing of the forelimb too. The angular morphology of the glenoid fossa suggests a moderate range of rotation of the humeral head within the glenoid cavity, which also agrees with a non-fully erected posture. Accordingly, sprawling or semi-erected posture are the most likely terrestrial locomotion model to be inferred in *A. hulki*.

Another important trait of the scapula of *A. hulki* is the presence of several rough surfaces related to muscular attachment. Especially noteworthy are those located in the anterior process of the scapula, such as the *M. supracoracoideus intemedius*, *M. supracoracoideus longus*, and *M. coracobrachialis brevis dorsalis,* which occupy relatively more surface than in extant crocodilomorph (Fig. 5A-C; see Meers, 2003). These muscles are primarily involved in stabilizing the shoulder joint, but they are also powerful protractor and adductor of the humerus, and may assist in the extension of the forelimb. The *M. deltoideus clavicularis*, another powerful protractor of the humerus, is not specially developed in *A. hulki*, but muscle insertions are strongly marked. As a result, the morphology and myology configuration of the scapula of *A. hulki* seems to point at a powerful shoulder, with strong protractor/adduction capacities capable to support a robust body, keeping it off the ground.

Like the scapula, the humerus has an overall robust aspect, and it could be relatively short (Fig. 5D-G). Because it lacks both epiphyseal ends, few assessments in regards to the torsion of the shaft or development of the articular parts can be performed. Furthermore, the preserved humerus does no exhibit any distinctive feature in its diaphysis if compared with extant crocodilians. Apart of the wide rough areas related to the *M. scapulohumeralis caudalis*, and the *triceps brachii* muscle complex, the

727 humerus is a nearly smooth (Fig. 5D-G). The *M. scapulohumeralis caudalis* assists in the elevation of
728 the humerus and its stabilization within the glenohumeral joint, but also plays an important role in the
729 protraction of the humerus. The main function of triceps brachii complex is to assist in the flexion of
730 the brachium on the shoulder while extending the antebrachium on the brachium, thus supporting the
731 body off the ground against gravity (Meers, 2003). These muscular features are in line with previous
732 ideas that suggest *A. hulki* could have robust forelimbs capable to perform powerful protractor
733 movements during terrestrial locomotion.
734 The ulna is the most distinctive element of the forelimb of *Allodaposuchus hulki*. It is featured by an
735 expanded proximal epiphysis with prominent processes, a shaft comprised mediolaterally with wide
736 grooves location in both medial and lateral sites, and a marked twist of the distal end of the shaft.
737 Overall, the ulna of *A. hulki* resembles those of extant crocodile taxa, but its expanded proximal
738 epiphysis and twisted distal part resemble that of *Simosuchus* and *Sebecus* (Sertch & Groenke, 2011).
739 As previously stated, the most prominent rugosity of the ulna is located in the olecranon process,
740 corresponding to the insertion of *M. triceps brachi* (Fig. 5H, I; Meers, 2003, Allen et al., 2014). Less
741 marked are those areas related with the insertion of *M. flexor ulnaris* and *M. pronator quadratus,*
742 though they occupy relatively more surface than in current crocodile taxa (see Meers, 2003). This
743 would mean that *A. hulki* could exhibit powerful muscles related to the flexion and pronation of the
744 antebrachium. The crest placed at the origin of the *M. flexor digitorium longus* also suggests a complex
745 mechanism involved in the flexion of the wrist. Although characteristics of the appendicular skeleton
746 suggest that *A. hulki* was not suited of fully erect posture, several features indicate powerful forelimb
747 capable to perform sprawling and semi-erected postures. Further, the robust configuration of the
748 forelimbs seems to be consistent with a terrestrial lifestyle, or semi-terrestrial, rather than semi-aquatic
749 one.
750 The semi-terrestrial lifestyle hypothesis for *Allodaposuchus hulki* is also supported by the high degree
751 of penumaticity observed in its skull. Although large cranial cavities of *A. hulki*, such as the caudal
752 tympanic recesses and quadrate sinuses, seem to be primarily related to a specialized otic system, they
753 could also play an important role in lightening the weight of the skull like in large non-avian theropods
754 (see Witmer et al., 2008; Witmer & Ridgey, 2009, 2010), or other terrestrial vertebrates.
755
756 **Ecological implications**

According to both crania and postcranial features displayed in *Allodaposuchus hulki*, it could exhibit some kind of terrestrial or semi-terrestrial life-style rather than semi-aquatic one. This interpretation is also supported by paleoenvironmental evidences.

Charophyte fructifications at the Casa Fabà outcrop were found in the grey claystones above the pedogenized channelized sandstone bed belonging to the lower part of the fluviatile 'lower red unit' (Riera et al., 2009). The charophyte assemblage is formed by extremely small gyrogonites of *Microchara cristata* Grambast 1971, *Microchara nana* Vicente & Martín-Closas 2015, *Microchara punctata* Feist & Colombo 1983 and *Microchara aff. laevigata* Grambast & Gutiérrez 1977. Most of the samples show well-preserved gyrogonites suggesting that they belong to an autochthonous assemblage. Charophytes were also found along to gastropod shells and operculi, fragmentary vertebrate remains and slightly eroded eggshells and planktonic foraminifera.

Assemblages formed exclusively by species bearing small gyrogonites (e.g. *M. nana)* have been related to turbid and warm ephemeral ponds usually found in terrigenic floodplains (Vicente et al., 2015). Despite being also common in lacustrine and palustrine environments, the absence of typically lacustrine species in the assemblages suggests that this highly fluctuant and stressed continental environment favor the thriving of these adapted species bearing small gyrogonites.

In addition, no channel or lake deposits have been found near the Casa Fabà site, or at least not closer than 2.5 km around. These evidences, along with anatomical characteristics, may suggest that *Allodaposuchus hulki* could perform relatively large incursion on earth, moving from place to place, only stopping in ephemeral water bodies looking for food or other resources.

Acknowledgments

We thank the staff of Museu de Ciències Naturals de Barcelona for the temporary loan of extant specimens for comparison, Hospital Universitari Mútua de Terrassa for the CT-scanning, the Preparation Division of the ICP for the preparation of the fossils specimens, Sergio Llácer for the image processing and the following curators or researchers for permission to study fossil material under their care: A.M. Bravo (Museo Geológico de Madrid, Madrid); R. Gaete (Museu de la Conca Dellà, Spain).

References

Allen V, Molnar J, Parker W, Pollard A, Nolan G, Hutchinson JR. 2014. Comparative architectural

788 properties of limb muscles in Crocodylidae and Alligatoridae and their relevance to divergent use of
789 asymmetrical gaits in extant Crocodylia. *Journal of Anatomy* 255:569-582.
790 Benton MJ, Clark JM. 1988. Archosaur phylogeny and the relationships of Crocodylia. In: Benton MJ,
791 ed. *The phylogeny and classification of the tetrapods*. Oxford: Clarendon Press 295-338.
792 Bierman HS, Thornton JL, Jones HG, Koka K, Young BA, Brandt C, Christensen-Dalsgaard J, Carr
793 CE, Tollin DJ. 2014. Biophysics of directional hearing in the American alligator (*Alligator*
794 *mississippiensis*). *The Journal of Experimental Biology* 217:1094-1107.
795 Blanco A, Puértolas-Pascual E, Marmi J, Vila B, Sellés AG. 2014. *Allodaposuchus palustris* sp. nov.
796 from the upper Cretaceous of Fumanya (south-eastern Pyrenees, Iberian Peninsula): systematics,
797 palaeoecology and palaeobiogeography of the enigmatic allodaposuchian crocodylians. *PLoS ONE*
798 12e115837.
799 Bona P, Degrange FJ, Fernández MS. 2013. Skull Anatomy of the bizarre crocodylian *Mourasuchus*
800 *nativus* (Alligatoridae, Caimaninae). *The Anatomical Record* 296:227-239.
801 Briknam D. 1980. Hind limb step cycle of *Caiman sclerop* and the mechanics of the crocodile tarsus
802 and metatarsus. *Canadian Journal of Zoology* 58: 2187-2200.
803 Brochu CA. 1997. Phylogenetic systematics and taxonomy of Crocodylia. *PhD dissertation*, Austin:
804 University of Texas.
805 Brochu CA. 2011. Phylogenetic relationships of *Necrosuchus ionensis* Simpson, 1937 and the early
806 history of caimanines. *Zoological Journal of the Linnean Society* 163:S228-S256.
807 Buscalioni AD, Ortega F, Vasse D. 1997. New crocodiles (Eusuchia: Alligatoroidea) from the Upper
808 Cretaceous of Southern Europe. *Comptes Rendus Académie des Sciencie de Paris* 325:525-530.
809 Buscalioni AD, Ortega F, Weishampel DB, Jianu CM. 2001. A revision of the crocodyliform
810 *Allodaposuchus precedens* from the Upper Cretaceous of the Haţeg Basin, Romania. Its relevance in
811 the phylogeny of Eusuchia. *Journal of Vertebrate Paleontology* 21:74-86.
812 Chamero B, Buscalioni AD, Marugán-Lobón J. 2013. Pectoral girdle and forelimb variation in extant
813 Crocodylia: the coracoid–humerus pair as an evolutionary module. *Biological Journal of the Linnean*
814 *Society* 108:600-618.
815 Dalla Vecchia FM, Gaete R, Riera V, Oms O, Prieto-Márquez A, Vila B, Garcia Sellés A, Galobart À.
816 2014. The Hadrosauroid Record in the Maastrichtian of the Eastern Tremp Syncline (Northern Spain)
817 In: Eberth DA, Evans DC, eds. *Hadrosaurs*. Bloomington and Indianapolis: Indiana University Press,
818 298-313.

819 Delfino M, Codrea V, Folie A, Dica P, Godefroit P. 2008. A complete skull of *Allodaposuchus*
820 *precedens* Nopcsa 1928 (Eusuchia) and a reassessment of the morphology of the taxon based on the
821 Romanian remains. *Journal of Vertebrate of Paleontology* 28:111-122.
822 Dollo L. 1883. Premiere note sur les crocodiliens de Bernissart. *Bulletin de l'Institut Royal des*
823 *Sciences Naturelles de Belgique* 2:309-338.
824 Dufeau DL, Witmer, LM. 2007. Ontogeny and phylogeny of the tympanic pneumatic system of
825 crocodyliform archosaurs. In *67th Annual Meeting Society of Vertebrate, Austin*, Abstract Volume, p.
826 70A.
827 Feist M, Colombo F. 1983. La limite Crétacé-Tertiaire dans le nord-est de l'Espagne, du point de vue
828 des charophytes. *Géologie Méditerranéenne* 10(3-4):303-326.
829 Fernández MS, Carabajal AP, Gasparini Z, Chong Díaz G. 2011. A metriorhynchid crocodyliform
830 braincase from northern Chile. *Journal of Vertebrate Paleontology* 31(2):369-377.
831 Gaete R. 2009. Sistemática y filogenia del hadrosáurido (Dinosauria, Ornithopoda) del yacimiento de
832 Basturs Poble (Pirineos sur-centrales, Isona i Conca Dellà, Lleida). *Master dissertacions*. Barcelona:
833 Universidad Autónoma de Barcelona.
834 Gatesy SM. 1991. Hind limb moviments of the American alligator (*Alligator mississippiensis*) and
835 postural grade. *Journal of Zoology* 224:557-588.
836 George ID, Holliday CM. 2013. Trigeminal nerve morphology in *Alligator mississippiensis* and its
837 significance for crocodyliform facial sensation and evolution. *The anatomical record* 296:670-680.
838 Gmelin JF. 1789. Caroli a Linné. Sistema Naturae per regna tri naturae: secundum classes, ordines,
839 genera, species, cum characteribus, differentiis, synonymis, locis. *Leipzig* 1(3):1033-1516.
840 Goloboff PA, Farris JS, Nixon KC. 2008a. TNT: a free program for phylogenetic analysis. *Cladistics*
841 24:774-786.
842 Grambast L. 1971. Remarques phylogénétiques et biochronologiques sur les *Septorella* du Crétacé
843 terminal de Provence et les charophytes associées. *Paléobiologie continentale* 2(2):1-38.
844 Grambast L, Gutiérrez G. 1977. Espèces nouvelles de charophytes du Crétacé supérieur terminal de la
845 province de Cuenca (Espagne). *Paléobiologie continentale* 8(2):1–34.
846 Hay OP. 1930. Second bibliography and catalogue of the fossil vertebrata of North America. *Carnegie*
847 *Institute Washington Publication* 390(2):1-1074.
848 Huxley TH. 1875. On *Stagonolepis robertsoni*, and on the evolution of the Crocodilia. *The quarterly*
849 *journal of the Geological Society of London* 31:423-438.

Iordansky N.N. 1973. The skull of the Crocodilia. In: Gans C, & Parsons TS, eds. *Biology of the Reptilia* Vol. 4*: Morphology*. London: Academic Press, 201–262.

Kley NJ, Sertich JJW, Turner AH, Krause DW, O'Connor PM, Georgi JA. 2010. Craniofacial Morphology of *Simosuchus clarki* (Crocodyliformes: Notosuchia) from the Late Cretaceous of Madagascar. *Journal of Vertebrate Paleontology* 30(s1):13-98.

Laurent Y, Buffetaut E, Le Loeuff J, 2000. Un crâne de Thoracosaurine (Crocodylia, Crocodylidae) dans leMaastrichtien supérieur du Sud de la France. *Oryctos* 3:19-27.

López-Martínez N, Vicens E. 2012. A new peculiar dinosaur egg, *Sankofa pyrenaica* oogen. nov. oosp. nov. from the upper cretaceous coastal deposits of the Aren Formation, South-Central Pyrenees, Lleida, Catalonia, Spain. *Palaeontology* 55(2):325–339.

Märsche I. 1996. European Mesozoic-Cenozoic charophyte biozonation. *Bulletin de la Société Géologique de France* 167:453–468.

Martin JE, Buffetaut E. 2008. *Crocodilus affuvelensis* Matheron, (1869) from the Late Cretaceous of southern France: a reassessment. *Zoological Journal of the Linnean Society* 152:567-580.

Martin JE, Delfino M. 2010. Recent advances in the comprehension of the biogeography of Cretaceous European eusuchians. *Palaeogeography, Palaeoclimatology, Palaeoecology* 293:406-418.

Martin J. 2010. *Allodaposuchus* Nopcsa 1928 (Crocodylia, Eusuchia), from the Late Cretaceous of southern France and its relationships to Alligatoroidea. *Journal of Vertebrate Paleontology* 30(3):756-767.

Meers MB. 2003. Crocodylian forelimb musculature and its relevance to Archosauria.
The Anatomical Record 274A(2):891–916.

Mook C. 1921. Notes on the postcranial skeleton in the Crocodilia. *Bulletin of the American Museum of the Natural History* Vol. XLIV.

Muñoz, JA, Martínez A, Vergés, J. 1986. Thrust sequence in the Spanish eastern Pyrenees. *Journal of Structural Geology* 8:399–405.

Narváez I, Ortega F, Brochu C, Escaso, F. 2014. Reevaluation of the phylogenetic status of the eusuchian crocodile *Musturzabalsuchus* from the Late Cretaceous of Spain. *Abstracts of papers of the 74th SVP Annual Meeting*, 194.

Nopcsa F. 1928. Paleontological notes on Reptilia. 7. Classification of the Crocodilia. *Geologica Hungarica, Series Palaeontologica* 1:75–84.

Ösi A, Clark JM, Weishampel DB. 2007. First report on a new basal eusuchian crocodyliform with

multi-cusped teeth from the upper cretaceous (Santonian) of Hungary. *Neues Jahrbuch* für Geologie und Paläontologie, *Abh* 243:169-177.

Parish JM. 1986. Locomotor adaptation in the hindlimb and pelvis of Thecodontia. *Hunteria* 1:1-35.

Parish JM. 1987. The origin of crocodilian locomotion. *Paleobiology* 13:396-414.

Pol D, Leardi JM, Lecuona A, Krause, M. 2012. Postcranial anatomy of *Sebecus icaeorhinus* (Crocodyliformes, Sebecidae) from the Eocene of Patagonia. *Journal of Vertebrate Paleontology* 32(2):328–354.

Puértolas E, Canudo JI, Cruzado-Caballero P. 2011. A new Crocodylian from the Late Maastrichtian of Spain: Implications for the initial radiation of crocodyloids. PLoS ONE 6(6): e20011. doi:10.1371/journal.pone.0020011.

Puértolas-Pascual E, Canudo JI, Moreno-Azanza M. 2013. The eusuchian crocodylomorph *Allodaposuchus subjuniperus* sp. nov., a new species from the latest Cretaceous (upper Maastrichtian) of Spain. *Historical Biology* **26:**91–109.

Puigdefàbregas C, Souquet P. 1986 Tectosedimentary cycles and depositional sequences of the Mesozoic and Tertiary from the Pyrenees. *Tectonophysics* 129:173–203.

Riera V, Oms O, Gaete R, Galobart À. 2009. The end-Cretaceous dinosaur succession in Europe: the Tremp Basin record (Spain). *Palaeogeography, Palaeoclimatology, Palaeoecology* 283:160-171.

Riveline J, Berger JP, Bilan W, Feist M, Martín-Closas C, Schudack M, Soulié-

Rosell J, Linares R, Llompart C. 2001. El "Garumniense" prepirenaico. *Revista de la Sociedad Geológica de España* 14:47-56.

Salisbury SW, Molnar RE, Frey E, Willis PMA. 2006. The origin of modern crocodyliforms: new evidence from the Cretaceous of Australia. *Proceedings of the Royal Society of London, Serie B* 273:2439-2448.

Sertch JJW, Groenke JR. 2011. Appendicular skeleton of Simosuchus clarki (Crocodyliformes: Notosuchia) from the Late Cretaceous of Madagascar. *Journal of Vertebrate Paleontology* 6:122-153.

Vicente A, Martín-Closas C, Arz JA, Oms O. 2015. Maastrichtian–basal Paleocene charophyte biozonation and its calibration to the Global Polarity Time Scale in the Southern Pyrenees (Catalonia, Spain). *Cretaceous Research* 52:268–285.

Vila B, Galobart À, Canudo JI, Le LoeufF J, Dinarès-Turell J, Riera V, Oms O, Tortosa T, Gaete R. 2012. The diversity of sauropod dinosaurs and their first taxonomic succession from the latest

911 Cretaceous strata of Southwestern Europe: clues to demise and extinction. *Palaeogeography,*
912 *Palaeoclimatology, Palaeoecology* 350-352:19–38.
913 Wharton DS. 2000. An enlarged endocranial venous system in Steneosaurus pictaviensis (Crocodylia:
914 Thalattosuchia) from the Upper Jurassic of Les Lourdines, France. *Comptes Rendus de l'Académie des*
915 *Sciences de Paris* 331:221–226.
916 Witmer LM, Ridgely RC. 2008. The paranasal air sinuses of predatory and armored dinosaurs
917 (Archosauria: Theropoda and Ankylosauria) and their contribution to cephalic architecture. *Anatomical*
918 *Record* 291:1362–1388.
919 Witmer LM, Ridgely RC. 2009. New insights into the brain, braincase, and ear region of *Tyrannosaurs*
920 (Dinosauria, Theropoda), with implications for sensory organization and behavior. *The anatomical*
921 *record* 292:1266-1296.
922 Witmer LM, Ridgely RC. 2010. The Cleveland tyrannosaur skull (*Nanotyrannus* or *Tyrannosaurus*):
923 new findings based on ct scanning, with special reference to the braincase. *Kirtlandia. The Cleveland*
924 *Museum of Natural History* 57:61-81.
925 Witmer LM, Ridgely RC, Dufeau DL, Semones MC. 2008. Using CT to peer into the past: 3D
926 visualization of the brain and ear regions of birds, crocodiles, and nonavian dinosaurs. In: Endo H,
927 Frey R, eds. *Anatomical Imaging: Towards a New Morphology*. Tokyo: Springer-Verlag. 67–88.
928
929 **Figure Captions**
930 **Figure 1.** Geographical and geological location of the Casa Fabà site. A) Geological map of the Tremp
931 Basin (modified from López-Martínez & Vicens, 2012); B) stratigraphical section performed near the
932 Casa Fabà site (modified from Riera et al., 2009); C) mapping of the crocodilian bones at the Casa
933 Fabà locality.
934 **Figure 2.** Skull of *Allodaposuchus hulki* sp. nov. (MCD5139) and interpretative diagrams in (A) dorsal,
935 (B) ventral, (C) caudal, and (D) left lateral view.
936 Abbreviations: bc, basicranium; ctp, *cavum tympanicum propium*; cqp, cranioquadrate passage; ex,
937 exoccipital; f, frontal; fa, *foramen aërum*; fm, *foramen magnum*; fo, foramen; gef, groove for ear flap;
938 la, lacrimal; lhc, lateral hemicondyle; ls, laterosphenoid; mhc, medial hemicondyle; olt, olfactory track;
939 orb, orbit; p, parietal; pf, prefrontal; po, postorbital; ptf, postemporal fenestrae; q, quadrate; so,
940 supraoccipital; sq, squamosal; stf, supratemporal fenestra.

941 **Figure 3.** Cranio-mandibular elements of *Allodaposuchus hulki* and interpretative diagrams. Left
942 premaxilla (MCD4763) in (A) dorsal, and (B) ventral view. Right dentary fragment (MCD5134) in (C)
943 labial view. Right pair jugal-quadratojugal (MCD5129) in (D) dorsolateral and (E) ventromedial view.
944 Indeterminate jaw fragment (MCD4758a) in (F) labial and (G) mesial view. Reconstruction of the skull
945 of *Allodaposuchus hukli* (H).
946 Abbreviation: al, alveoli; bpob, base of the postorbital bar; dal, dentary alveoli; dct, dentary caniniform
947 thooth; drt, dentary replacement tooth; fo, foramen; ids, interdentary septa; if, incisive foramen; j,
948 jugal; j-m, jugal-maxilla suture; mjf, medial jugal foramen; op, occlusion pits; pmal, premaxillary
949 alveoli; pm-m, premaxilla-maxilla suture; pmt, premaxillary tooth; px-sy, premaxilla symphysis; qj,
950 quadratojugal; qj-q, quadratojugal-quadrate suture; qjs, quadratojugas spine, t, tooth.
951 **Figure 4.** Appendicular forelimb elements of *Allodaposuchus hulki* and interpretative diagrams. Right
952 scapula (MCD4760) in (A) medial, (B) anterior, (C) lateral, and (D) ventral view. Right humerus
953 (MCD4758b) in (E) ventral, (F) medial, (G) dorsal, and (H) lateral view. Right ulna (MCD4760) in (I)
954 medial, (J) lateral, (K) proximal, and (L) distal view.
955 Abbreviation: ap, anterior process; dacu, distal anterior condyle of the ulna; dc, deltoid crest; dpc,
956 deltopectoral crest; dpcu, distal posterior condyle of the ulna; fo, foramen; gl, glenoid; glf, glenoid
957 fossa; gr, groove; lap, lateral anterior process; map, medial anterior process; mc, medial crest; mgr,
958 medial groove; ol, olecranon; pcd, posterior circular depression; sb, scapular blade; sc-co, scapula-
959 coracoid suture;
960 **Figure 5**. Muscular map of the forelimb bones of *Allodaposuchus hulki*. Right scapula (MCD4760; A-
961 C), right humerus (MCD4758b, D-G), right ulna (MCD 4760, H-I); and reconstruction of the anterior
962 limb configuration (J). Muscle origins are indicated in pinky and insertions in blue.
963 Abbreviations: br, *M. brachialis*; cbd, *M. coracobrahialis brevis dorsalis*; dc, *M. deltoideus*
964 *clavicularis*; ds, *M. deltoideus scapularis*; ecrd-pu, *M. extensor carpi radialis brevis-pars ulnaris*; fdl,
965 *M. flexor digitorum longus*; fu, *M. flexor ulnaris*; hr, M. humeroradialis; ld, *M. latissum dorsi*; ls, *M.*
966 *levator scapulae*; pq, *M. pronator quadratus*; shc, *M. scapulohumeralis caudalis*; sci, *M.*
967 *supracoracoideus intermedius*; ss, *M. subscapularis*; svt, *M. serratus ventralis thoracis*; tb, *M. triceps*
968 *brachii*; tbc, *M. triceps brevis caudalis*; tbi, *M. triceps brevis intermedius*; tlc, *M. triceps longus*
969 *caudalis*; tm, *M. teres major;* tll, *M. triceps longus lateralis*;
970 **Figure 6.** Axial elements of *Allodaposuchus hulki* and interpretative diagrams. Anterior dorsal vertebra
971 (MCD5131) in (A) anterior, (B) posterior, (C) dorsal, and (D) left lateral view; first lumbar vertebra

(MCD5136) in (E) anterior, (F) posterior, (G) dorsal, and (H) left lateral view; second lumbar vertebra (MCD4769) in (I) anterior, (J) posterior, (K) dorsal, and (L) left lateral view; third lumbar vertebra (MCD5126) in (M) anterior, (N) posterior, (O) dorsal, and (P) left lateral view.

Abbreviations: aas, anterior articular surface; di, diapophysis; fo, foramen; hy, hypapophysis; nc, neural channel; ns, neural spine, par, parapophysis; poc, posterior condyle; poz, postzygapophysis; prz, prezygapophysis.

Figure 7. Cranial endocast and pneumatic sinuses within the semi-transparent body skull of *Allodaposuchus hulki* (MCD5139), derived from surface rendering of CT scan data in (A) dorsal, (B) ventral, (C) caudal, and (D) left lateral view. E) Detail of the braincase and cranial nerves; the inner ear is removed because obscured some endocast details.

Abbreviations: adtr, anterodorsal tympanic recess; cer, cerebral hemisphere; cn, cranial nerves; cqp, craniocuadrate passage; ctp, *cavum tympanicum propium*; ctr, caudal tympanic recess; dls, dorsal line dural venous, dtr, dorsal tympanic recess; ie, inner ear; itr, intertympanic recess; ob, olfactory bulb; ot, olfactory track; qs, quadrate sinus; sps, sphenoparietal dural venous. Cranial nerve identification: III, oculomotor nerve canal; IV, trochlear nerve canal; V1, opthalmig nerve canal; V2, maxillary nerve canal; V3, mandibular nerve canal; VI, abducens nerve canal; XII, hypoglossal nerve canal.

Figure 8. Resulting strict consensus cladogram illustrating the phylogenetic relationship of *Allosaposuchus hulki* and the basal position of ‘Allodaposuchia’ within Crocodylia. Values above nodes represent bootstrap percentage, whereas values under nodes represent Bremer support values.

Figure 1(on next page)

Geographical and geological location of the Casa Fabà site.

A) Geological map of the Tremp Basin (modified from López-Martínez & Vicens, 2012); B) stratigraphical section performed near the Casa Fabà site (modified from Riera et al., 2009); C) mapping of the crocodilian bones at the Casa Fabà locality.

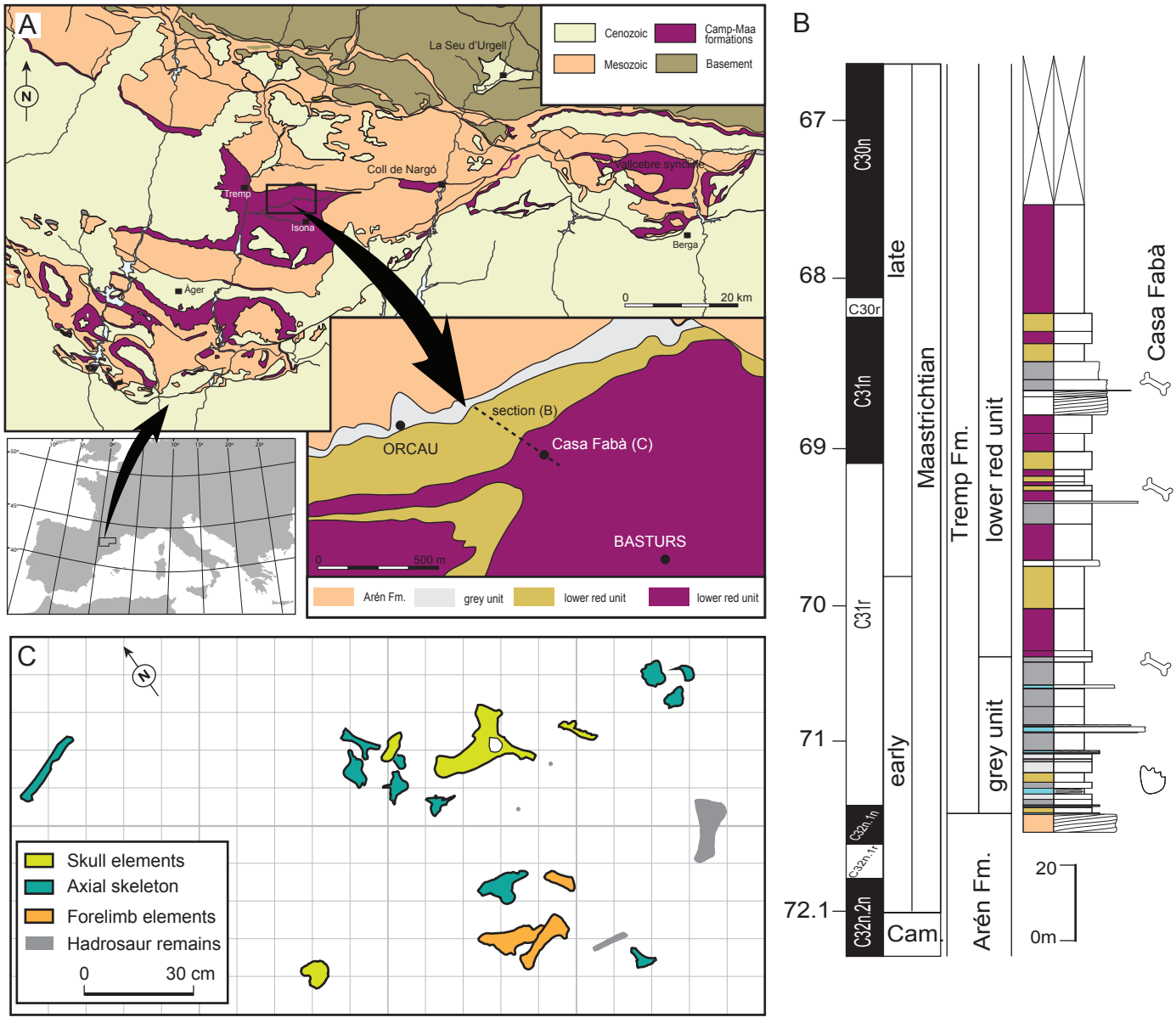
A
Cenozoic
Mesozoic
Camp-Maa formations
Basement
La Seu d'Urgell
Coll de Nargó
Tremp
Isona
Àger
Berga
0
20 km
section (B)
ORCAU
Casa Fabà (C)
BASTURS
0
500 m
Arén Fm.
grey unit
lower red unit
lower red unit
B
67
68
69
70
71
72.1
C30n
C30r
C31n
C31r
C32n.1n
C32n.1r
C32n.2n
late
early
Maastrichtian
Cam.
Tremp Fm.
lower red unit
grey unit
Arén Fm.
Casa Fabà
20
0m
C
Skull elements
Axial skeleton
Forelimb elements
Hadrosaur remains
0
30 cm

Figure 2(on next page)

Skull of *Allodaposuchus hulki* sp. nov.

(MCD5139) and interpretative diagrams in (A) dorsal, (B) ventral, (C) caudal, and (D) left lateral view. Abbreviations: bc, basicranium; ctp, *cavum tympanicum propium*; cqp, cranioquadrate passage; ex, exoccipital; f, frontal; fa, *foramen aërum*; fm, *foramen magnum*; fo, foramen; gef, groove for ear flap; la, lacrimal; lhc, lateral hemicondyle; ls, laterosphenoid; mhc, medial hemicondyle; olt, olfactory track; orb, orbit; p, parietal; pf, prefrontal; po, postorbital; ptf, postemporal fenestrae; q, quadrate; so, supraoccipital; sq, squamosal; stf, supratemporal fenestra.

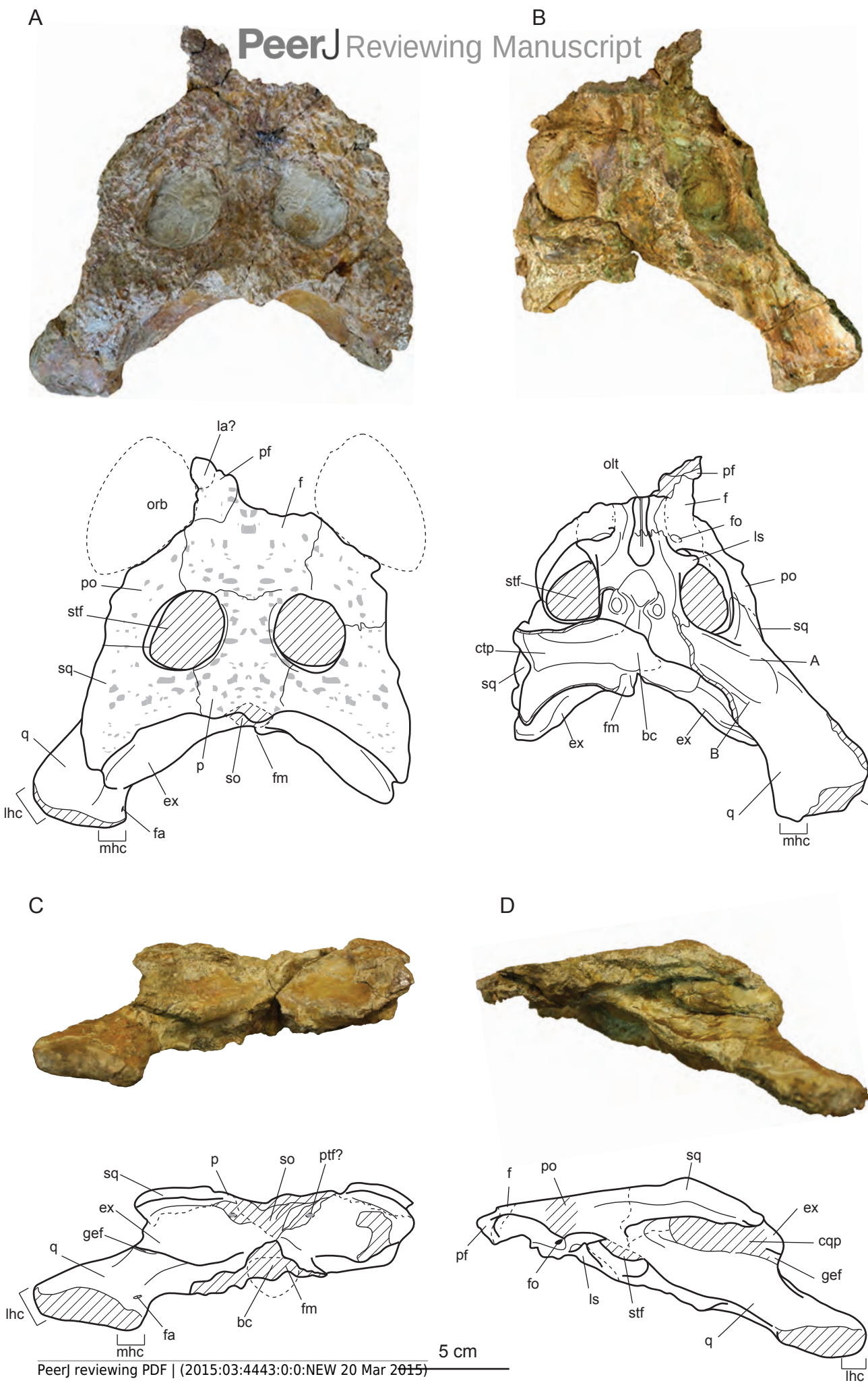

Figure 3(on next page)

Cranio-mandibular elements of *Allodaposuchus hulki* and interpretative diagrams.

Left premaxilla (MCD4763) in (A) dorsal, and (B) ventral view. Right dentary fragment (MCD5134) in (C) labial view. Right pair jugal-quadratojugal (MCD5129) in (D) dorsolateral and (E) ventromedial view. Indeterminate jaw fragment (MCD4758a) in (F) labial and (G) mesial view. Reconstruction of the skull of *Allodaposuchus hukli* (H). Abbreviation: al, alveoli; bpob, base of the postorbital bar; dal, dentary alveoli; dct, dentary caniniform thooth; drt, dentary replacement tooth; fo, foramen; ids, interdentary septa; if, incisive foramen; j, jugal; j-m, jugal-maxilla suture; mjf, medial jugal foramen; op, occlusion pits; pmal, premaxillary alveoli; pm-m, premaxilla-maxilla suture; pmt, premaxillary tooth; px-sy, premaxilla symphysis; qj, quadratojugal; qj-q, quadratojugal-quadrate suture; qjs, quadratojugas spine, t, tooth.

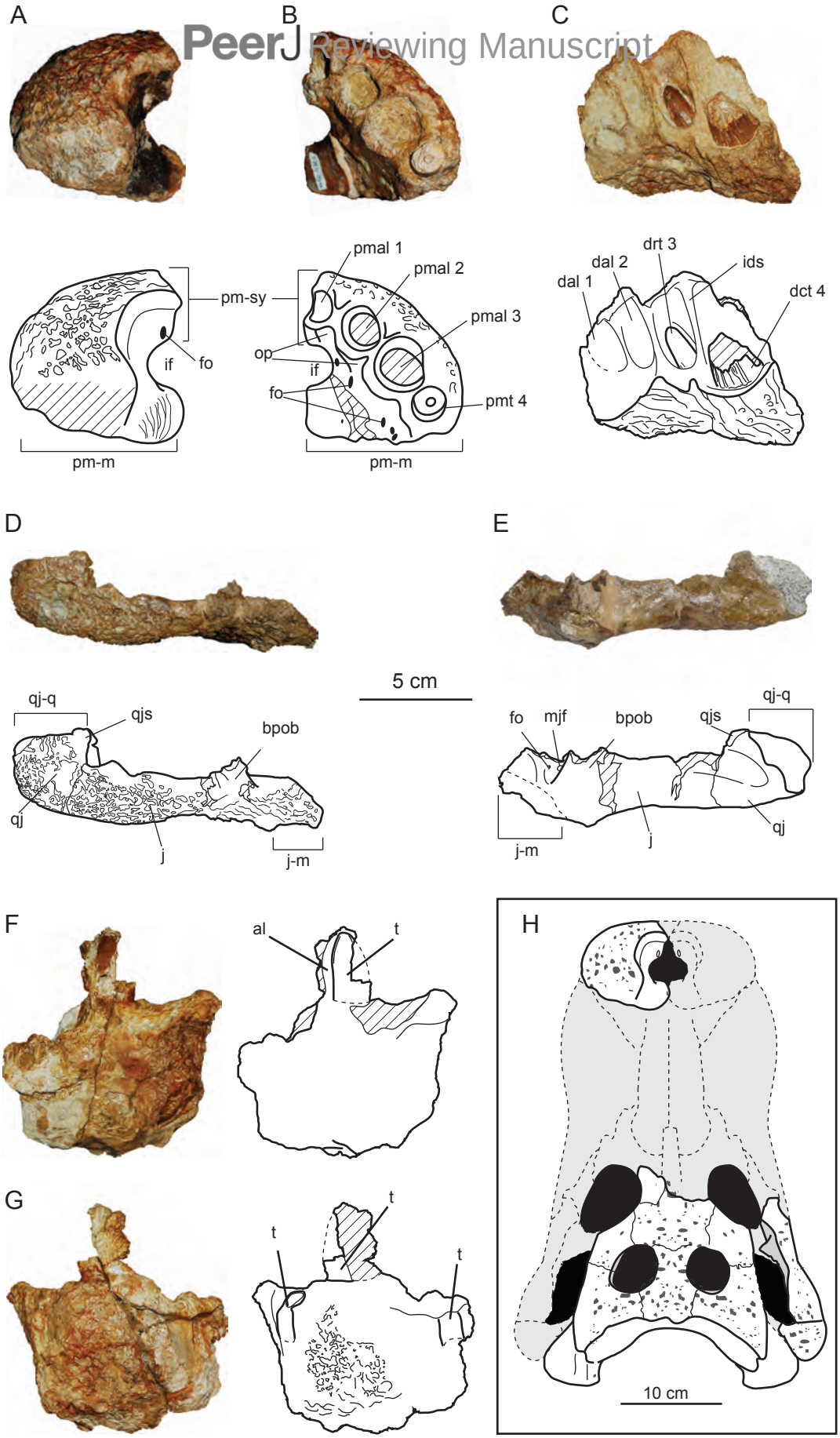

Figure 4(on next page)

Appendicular forelimb elements of *Allodaposuchus hulki* and interpretative diagrams.

Right scapula (MCD4760) in (A) medial, (B) anterior, (C) lateral, and (D) ventral view. Right humerus (MCD4758b) in (E) ventral, (F) medial, (G) dorsal, and (H) lateral view. Right ulna (MCD4760) in (I) medial, (J) lateral, (K) proximal, and (L) distal view. Abbreviation: ap, anterior process; dacu, distal anterior condyle of the ulna; dc, deltoid crest; dpc, deltopectoral crest; dpcu, distal posterior condyle of the ulna; fo, foramen; gl, glenoid; glf, glenoid fossa; gr, groove; lap, lateral anterior process; map, medial anterior process; mc, medial crest; mgr, medial groove; ol, olecranon; pcd, posterior circular depression; sb, scapular blade; sc-co, scapula-coracoid suture.

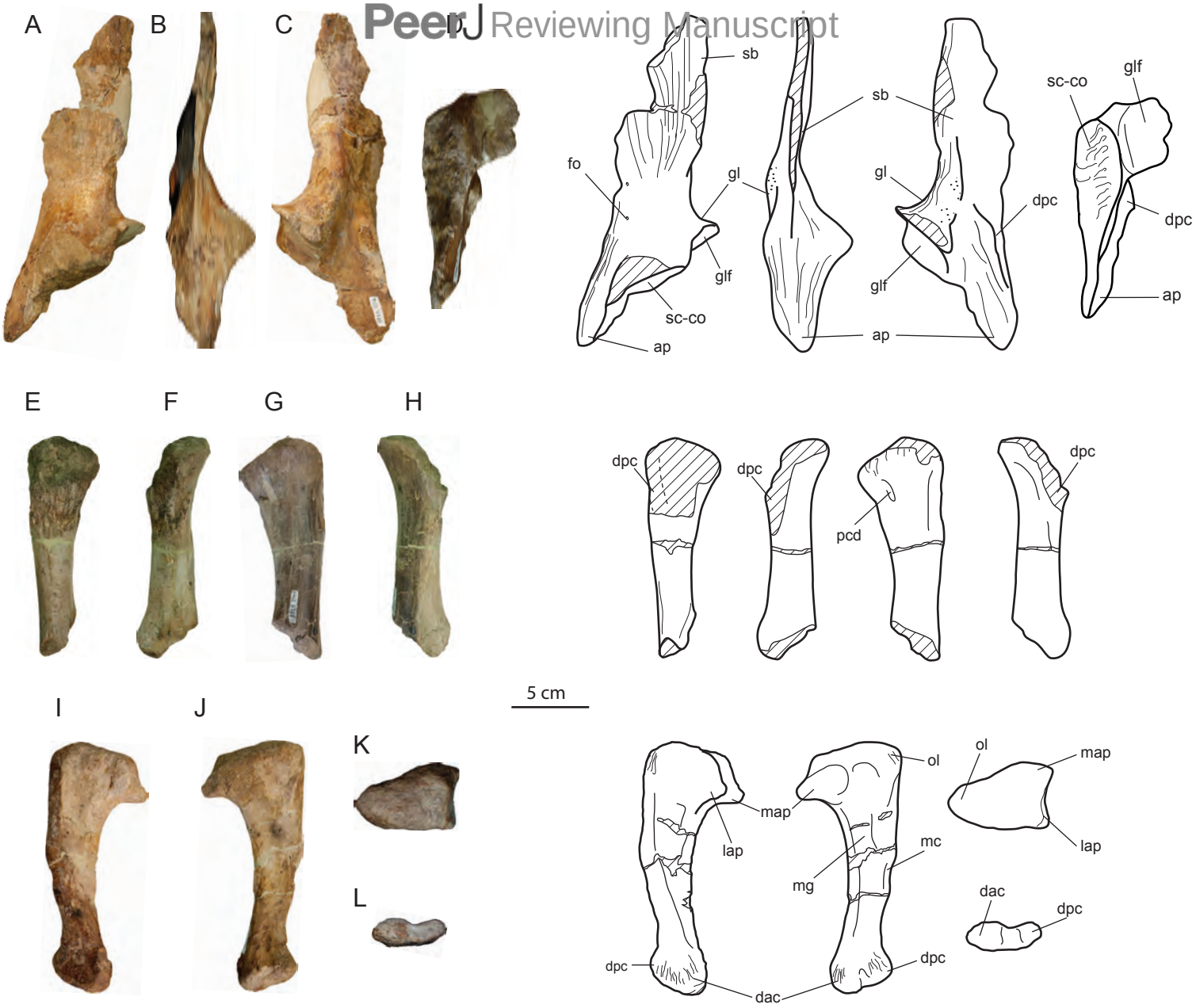

Figure 5(on next page)

Muscular map of the forelimb bones of *Allodaposuchus hulki*.

Right scapula (MCD4760; A-C), right humerus (MCD4758b, D-G), right ulna (MCD 4760, H-I); and reconstruction of the anterior limb configuration (J). Muscle origins are indicated in pinky and insertions in blue. Abbreviations: br, *M. brachialis*; cbd, *M. coracobrahialis brevis dorsalis*; dc, *M. deltoideus clavicularis*; ds, *M. deltoideus scapularis*; ecrd-pu, *M. extensor carpi radialis brevis-pars ulnaris*; fdl, *M. flexor digitorum longus*; fu, *M. flexor ulnaris*; hr, M. humeroradialis; ld, *M. latissum dorsi*; ls, *M. levator scapulae*; pq, *M. pronator quadratus*; shc, *M. scapulohumeralis caudalis*; sci, *M. supracoracoideus intermedius*; ss, *M. subscapularis*; svt, *M. serratus ventralis thoracis*; tb, *M. triceps brachii*; tbc, *M. triceps brevis caudalis*; tbi, *M. triceps brevis intermedius*; tlc, *M. triceps longus caudalis*; tm, *M. teres major;* tll, *M. triceps longus lateralis.*

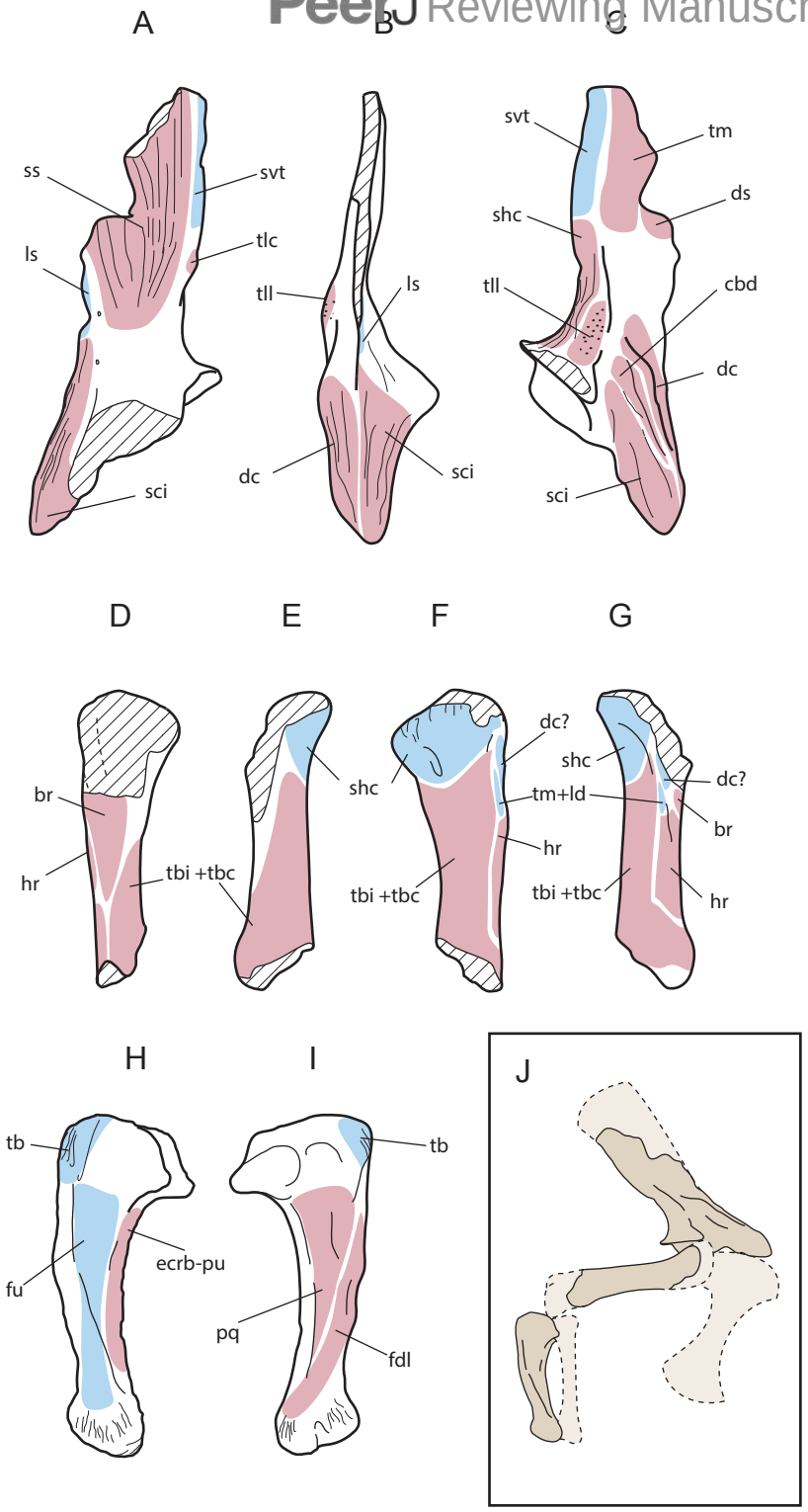
A
ss
svt
ls
tlc
sci
B
tll
ls
dc
sci
C
svt
tm
ds
shc
tll
cbd
dc
sci
D
br
hr
tbi +tbc
E
shc
F
dc?
shc
tm+ld
hr
tbi +tbc
G
dc?
br
tbi +tbc
hr
H
tb
ecrb-pu
fu
I
tb
pq
fdl
J

Figure 6(on next page)

Axial elements of *Allodaposuchus hulki* and interpretative diagrams.

Anterior dorsal vertebra (MCD5131) in (A) anterior, (B) posterior, (C) dorsal, and (D) left lateral view; first lumbar vertebra (MCD5136) in (E) anterior, (F) posterior, (G) dorsal, and (H) left lateral view; second lumbar vertebra (MCD4769) in (I) anterior, (J) posterior, (K) dorsal, and (L) left lateral view; third lumbar vertebra (MCD5126) in (M) anterior, (N) posterior, (O) dorsal, and (P) left lateral view. Abbreviations: aas, anterior articular surface; di, diapophysis; fo, foramen; hy, hypapophysis; nc, neural channel; ns, neural spine, par, parapophysis; poc, posterior condyle; poz, postzygapophysis; prz, prezygapophysis.

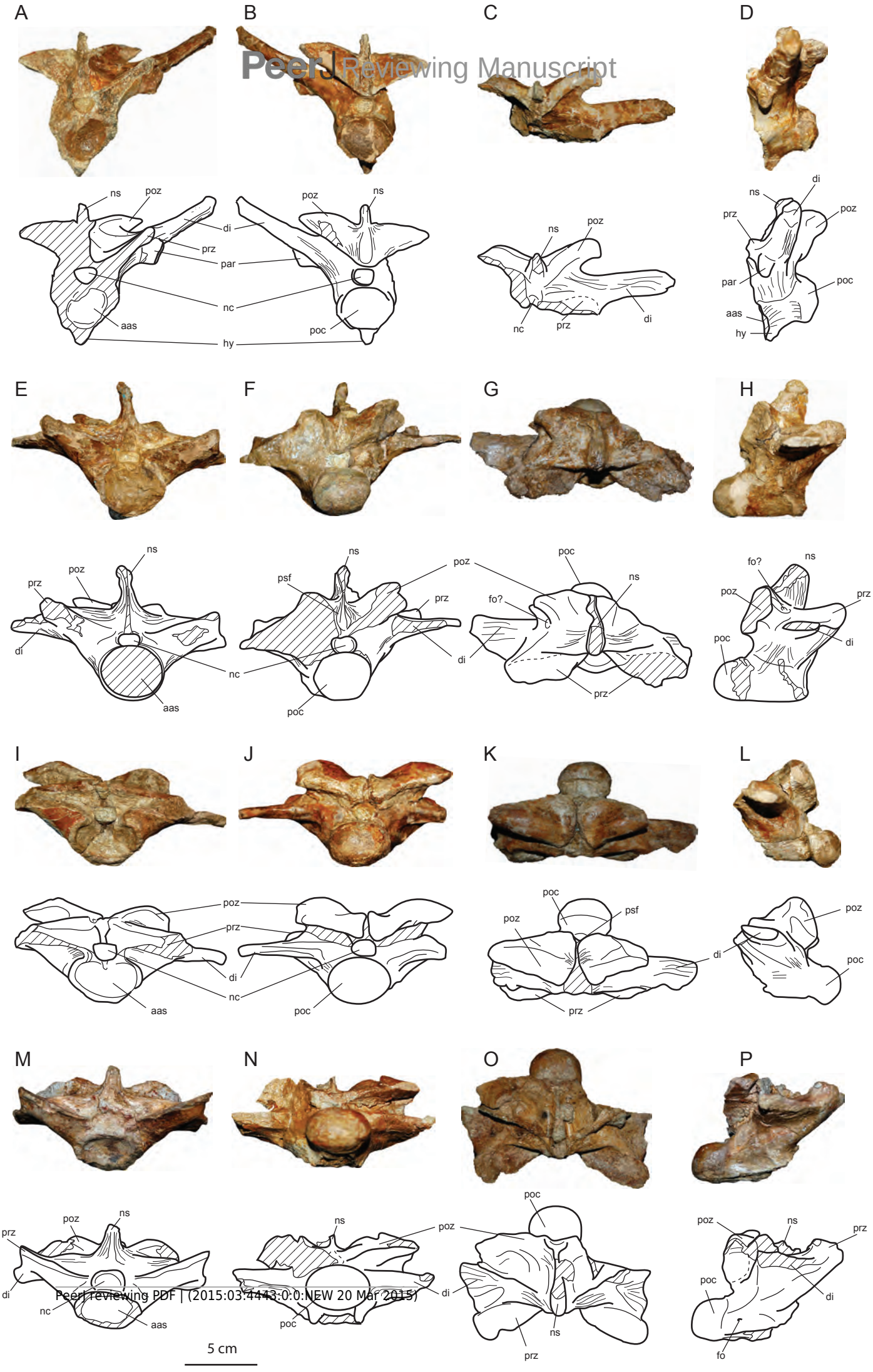

Figure 7 (on next page)

Cranial endocast and pneumatic sinuses within the semi-transparent body skull of *Allodaposuchus hulki.*

MCD5139 derived from surface rendering of CT scan data in (A) dorsal, (B) ventral, (C) caudal, and (D) left lateral view. E) Detail of the braincase and cranial nerves; the inner ear is removed because obscured some endocast details. Abbreviations: adtr, anterodorsal tympanic recess; cer, cerebral hemisphere; cn, cranial nerves; cqp, craniocuadrate passage; ctp, *cavum tympanicum propium*; ctr, caudal tympanic recess; dls, dorsal line dural venous, dtr, dorsal tympanic recess; ie, inner ear; itr, intertympanic recess; ob, olfactory bulb; ot, olfactory track; qs, quadrate sinus; sps, sphenoparietal dural venous. Cranial nerve identification: III, oculomotor nerve canal; IV, trochlear nerve canal; V1, opthalmig nerve canal; V2, maxillary nerve canal; V3, mandibular nerve canal; VI, abducens nerve canal; XII, hypoglossal nerve canal.

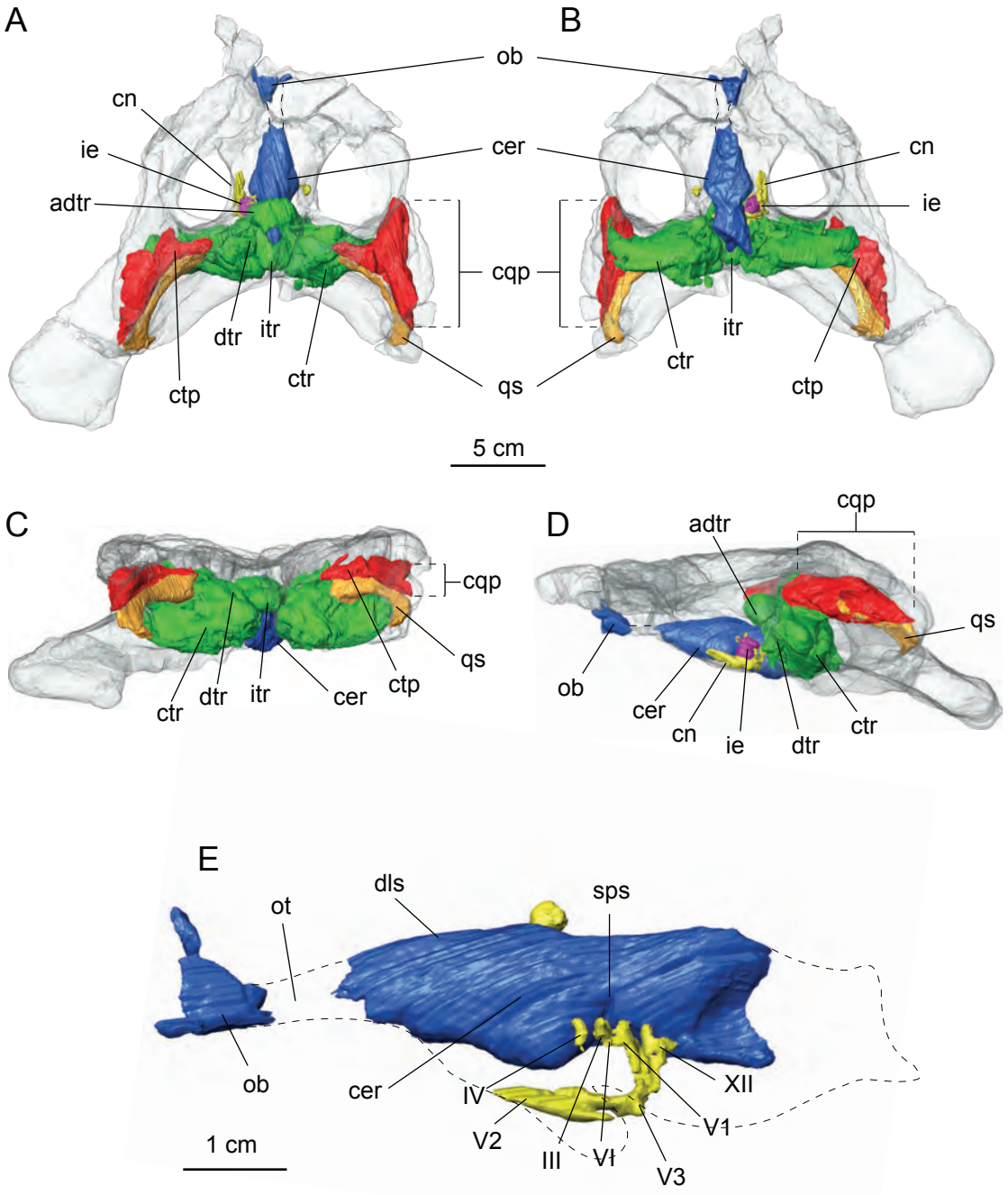
A
B
ob
cn
ie
cer
adtr
cqp
dtr
itr
ctr
ctp
qs
5 cm
C
D
cqp
adtr
qs
ob
cer
cn
ie
dtr
ctr
E
dls
ot
sps
ob
cer
IV
XII
V1
V2
III
VI
V3
1 cm

Figure 8(on next page)

Resulting strict consensus cladogram illustrating the phylogenetic relationship of *Allosaposuchus hulki* and the basal position of 'Allodaposuchia' within Crocodylia.

Values above nodes represent bootstrap percentage, whereas values under nodes represent Bremer support values.